iScience

CellPress
OPEN ACCESS

Article

RNA-modifying enzyme Alkbh8 is involved in mouse embryonic development

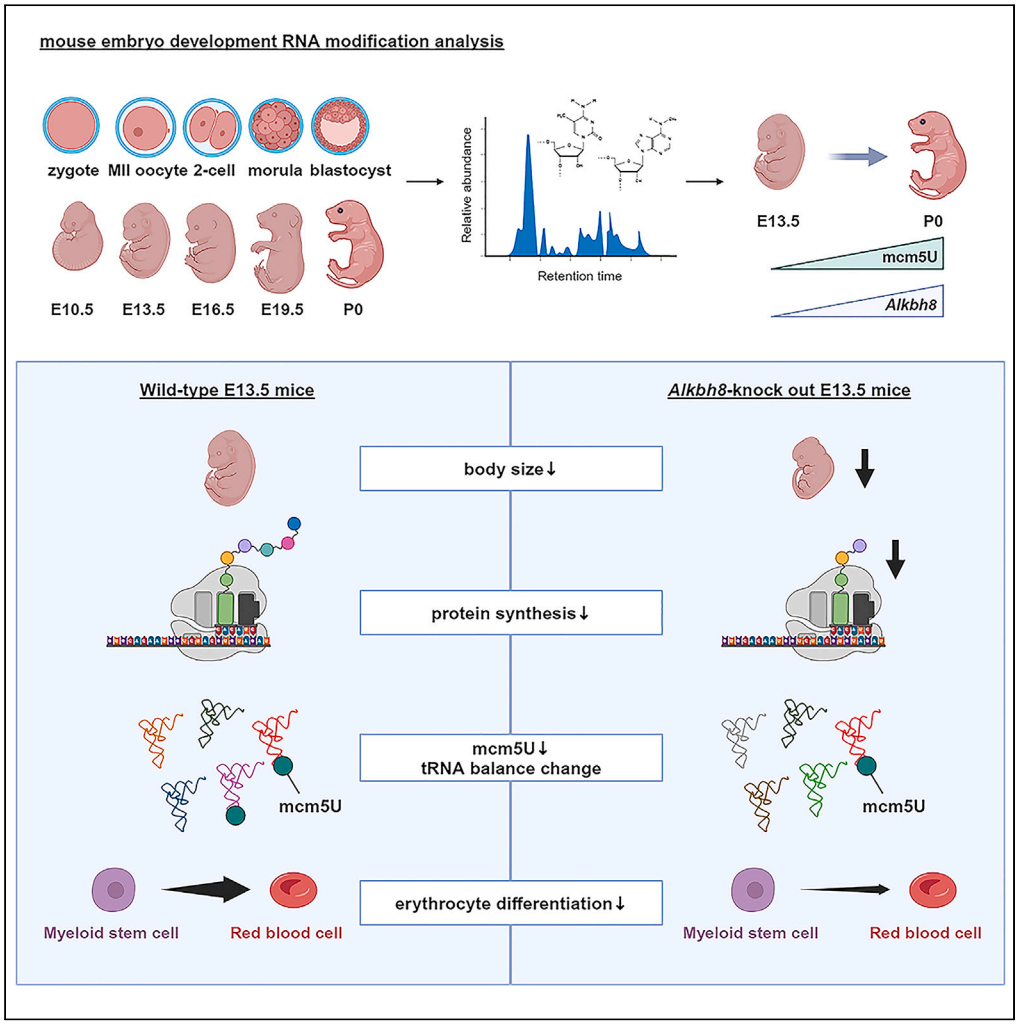

Manami Nakai, Hiroaki Hase, Yutong Zhao, ..., Kaori Ikuma, Kaori Kitae, Kazutake Tsujikawa

hase-h@phs.osaka-u.ac.jp

Highlights

RNA modification mcm5U and the mcm5U-modifying enzyme Alkbh8 increase after E13.5

In Alkbh8-KO mice, a decrease in body size was observed after E13.5

In Alkbh8-KO E13.5 mice, the cytoplasmic and mitochondrial tRNA balance was altered

Alkbh8 is essential for normal erythrocyte differentiation at E13.5

Nakai et al., iScience 27, 110777
September 20, 2024
https://doi.org/10.1016/j.isci.2024.110777

iScience

CellPress
OPEN ACCESS

Article

RNA-modifying enzyme Alkbh8 is involved in mouse embryonic development

Manami Nakai,[1] Hiroaki Hase,[1,2,*] Yutong Zhao,[1] Katsuya Okawa,[1] Kohei Honda,[1] Kaori Ikuma,[1] Kaori Kitae,[1] and Kazutake Tsujikawa[1]

SUMMARY

RNAs undergo more than 300 modifications after transcription. Aberrations in RNA modifications can lead to diseases; their involvement in fetal development has been suggested. This study explored the RNA modifications related to fetal development in mice. We quantified changes in RNA modifications present in mouse embryos at each stage: Metaphase II (MII) oocyte; pronucleus; 2-cell; morula; blastocyst; embryonic days (E)10.5, 13.5, 16.5, and 19.5; and newborn (post-natal day [P]0) using ultra-performance liquid chromatography-tandem mass spectrometry (UPLC-MS/MS). Our results confirm that many RNAs undergo dynamic modifications. In particular, 5-methoxycarbonylmethyluridine (mcm5U) modification was distinctive and increased during the fetal period. In *Alkbh8*-knockout (KO) mice, the tRNA protein translation efficiency was reduced. Proteome analysis revealed that the factors downregulated in *Alkbh8*-KO mice were associated with red blood cell and protoporphyrin metabolism. Our results suggest that ALKBH8 facilitates changes in tRNA balance in conjunction with mcm5U, which are essential for normal red blood cell differentiation and embryogenesis in mice.

INTRODUCTION

Since the discovery of pseudouridine as the fifth nucleoside of RNA in the 1950s,[1] over 300 diverse RNA modifications have been reported. These modifications include monomethylation, dimethylation, 2′-*O*-methylation of ribose, acetylation, and amino acid addition. Numerous modifications were initially discovered in tRNA.[2] Historically, RNA modifications were believed to contribute to the structural stabilization of RNA.[3]

Recent advances in developing antibodies against modified bases and transcriptome analyses using next-generation sequencers[4,5] have gradually revealed the physiological functions of RNA modifications. With advances in the technology for analyzing these RNA modifications, RNA modified by methylation and demethylation by intracellular enzymes changes higher-order structures and binds to RNA-binding proteins. These changes alter RNA stability, localization, and targets, indirectly controlling protein translation.[5–13] For instance, N6-methyladenosine (m6A), present with high frequency around the stop codon and the 5′ untranslated region in mRNA, is reversibly controlled *in vivo*.[5,6] The enzymes responsible for m6A methylation include methyltransferase-like protein (METTL)3/14[7], and the demethylases include fat mass and obesity-associated gene (FTO)[8] and AlkB homolog 5 (ALKBH5).[9] The YT521-B homology (YTH) family (YTHDF1-3, YTHDC1/2) has been identified as m6A-binding proteins through the YTH domain.[10] These m6A regulatory proteins regulate RNA stability, protein translation efficiency, RNA higher-order structure, intracellular localization, mRNA-selective polyadenylation, and splicing.[10–13] Furthermore, abnormalities in mRNA modifications have been reported to cause diseases, such as cancer,[14–19] drawing attention to the association between mRNA modifications and diseases.

Research on tRNA modifications surged in recent years, extending beyond the confines of mRNA studies.[20,21] These modifications are predominantly localized within tRNA molecules' anticodon and body regions (D-loop or T-loop). The base pairing between the first position (position 34) of tRNA's anticodon and the codon is known as "wobble pairing." Unlike Watson-Crick base pairing, wobble pairing is versatile and enables the selection of tRNAs to interpret multiple sense codons. Position 34 of the anticodon, pivotal for wobble pairing, hosts various wobble modifications that modulate codon recognition and protein synthesis.[22] For example, in the cytoplasmic tRNA of eukaryotes, 5-methoxycarbonylmethyluridine and its derivative 5-methoxycarbonylmethyl-2-thiouridine (mcm5s2U) exist at position 34. It has been reported that mcm5U modification, mediated by the mcm5U modification enzyme Alkbh8, controls selenoprotein synthesis.[23] The elongator acetyltransferase complex subunit (ELP)1 generates mcm5U at position 34 in cytoplasmic tRNA.[24–26] *Elp1*-knockout (KO) mice show embryonic lethality at embryonic day (E)10, likely due to impaired cardiovascular development and function, indicating an essential role of mcm5U in animal development.[27]

[1]Laboratory of Molecular and Cellular Physiology, Graduate School of Pharmaceutical Sciences, Osaka University, 1- 6 Yamadaoka, Suita, Osaka 565-0871, Japan
[2]Lead contact
*Correspondence: hase-h@phs.osaka-u.ac.jp
https://doi.org/10.1016/j.isci.2024.110777

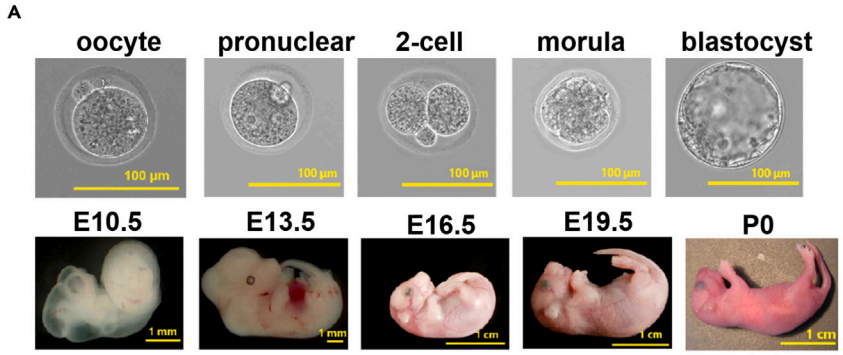
A
oocyte
pronuclear
2-cell
morula
blastocyst
100 μm
E10.5
E13.5
E16.5
E19.5
P0
1 mm
1 cm

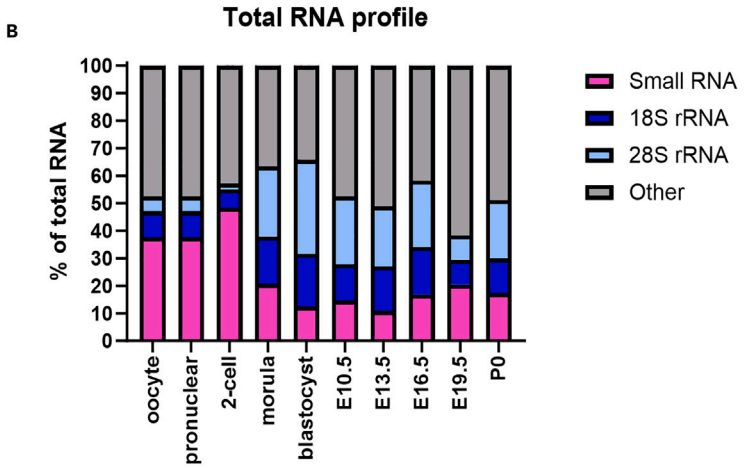
B
Total RNA profile
% of total RNA
Small RNA
18S rRNA
28S rRNA
Other
oocyte
pronuclear
2-cell
morula
blastocyst
E10.5
E13.5
E16.5
E19.5
P0

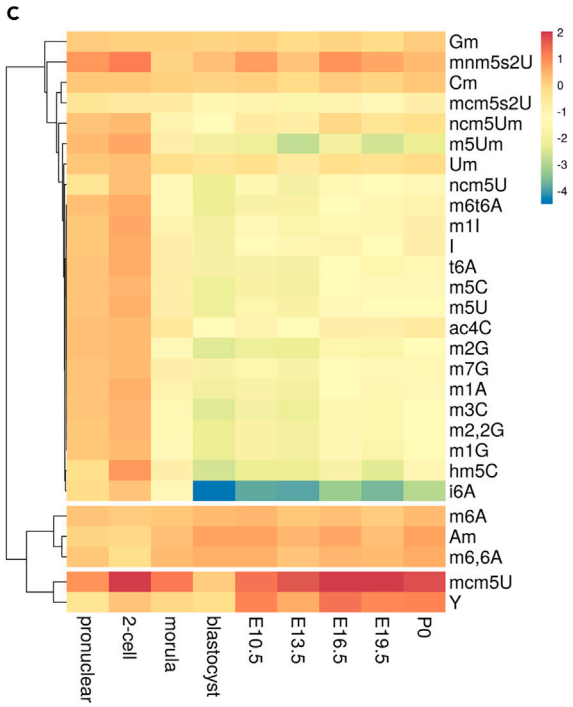
C
Gm
mnm5s2U
Cm
mcm5s2U
ncm5Um
m5Um
Um
ncm5U
m6t6A
m1I
I
t6A
m5C
m5U
ac4C
m2G
m7G
m1A
m3C
m2,2G
m1G
hm5C
i6A
m6A
Am
m6,6A
mcm5U
Y
pronuclear
2-cell
morula
blastocyst
E10.5
E13.5
E16.5
E19.5
P0

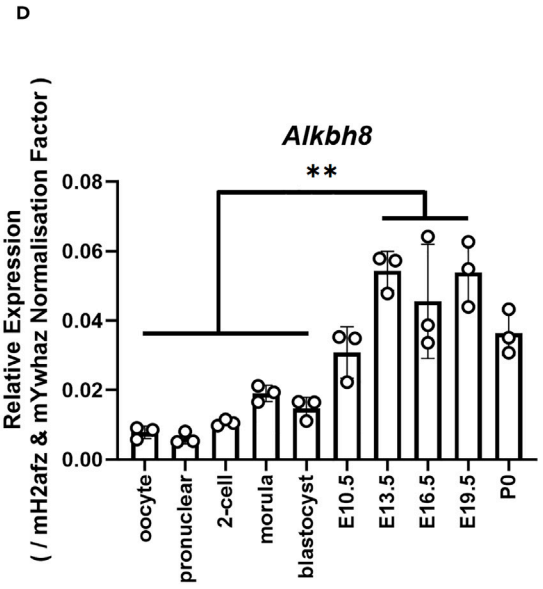
D
Alkbh8
**
Relative Expression
(/ mH2afz & mYwhaz Normalisation Factor)
0.08
0.06
0.04
0.02
0.00
oocyte
pronuclear
2-cell
morula
blastocyst
E10.5
E13.5
E16.5
E19.5
P0

Figure 1. The behavior of the RNA modification mcm5U was distinctive during the mouse developmental process

(A) Representative images of individual mice at each developmental stage. A scale bar is included in the photograph (MII oocyte, pronuclear, 2-cell, morula, and blastocysts: 100 μm; E10.5, E13.5, E16.5, E19.5, and P0: 1 cm).

(B) Total RNA profile at each developmental stage. The data represent the average values for MII oocytes, pronuclear, 2-cell, morula, and blastocysts: $n = 2$; E10.5, E13.5, E16.5, E19.5; and P0: $n = 3$. "Other" includes RNA fragments and mRNA, among other components. See Figure S1.

(C) Heatmap illustrating RNA modification changes relative to MII oocytes present in total RNA at each developmental stage, using representative values and the ratio of MII oocytes. MII oocytes, pronuclear, 2-cell, morula, and blastocyst: triplicates of pooled samples; E10.5, E13.5, E16.5, E19.5, and P0: three mice. The formal names of the RNA modifications are shown in Table S2.

(D) *Alkbh8* mRNA expression at each developmental stage. Data are represented as mean ± SD, MII oocytes, pronuclear, 2-cell, morula, and blastocyst: triplicates of pooled samples; E10.5, E13.5, E16.5, E19.5, and P0: three mice. $^{**}p < 0.01$ by one-way ANOVA with Tukey's multiple comparison test.

Mitochondrial tRNA (mitotRNA)at the anticodon position 34 contains 5-formylcytidine (f5C). Deficiencies in the f5C modification enzymes NOP2/Sun RNA methyltransferase 3(NSUN3) and ALKBH1 result in aberrant f5C modification.[20] This anomaly results in a marked decline in mitochondrial protein synthesis, culminating in diminished mitochondrial activity.[28,29] The absence of the 5-taurinomethyluridine modification in the anticodon loop of mitotRNA has been implicated as a causative factor in mitochondrial diseases.[30]

The tRNA's body region is crucial for maintaining the stability of its secondary and tertiary structures.[31] 5-methylcytidine (m5C) in tRNA is regulated by DNA methyltransferase 2 (DNMT2) and NOP2/Sun RNA methyltransferase 2 (NSUN2). Under conditions of stress or inhibition of DNMT2 and NSUN2, m5C in tRNA decreases. This reduction leads to tRNA degradation and a decrease in protein synthesis rate. Abnormal m5C modifications in tRNA have been reported to cause neurodevelopmental disorders.[32–34]

As illustrated earlier, RNA modifications, encompassing those in mRNA and tRNA, enrich the RNA repertoire and orchestrate pivotal physiological functions in organisms.

Research on RNA modifications related to development is progressing gradually. Studies have reported that m6A methylation in the mRNA of transcription factors related to pluripotency maintenance, such as *Nanog*, regulates mRNA turnover and controls fetal development in *Mettl3*-KO mice or cells.[35–37] In addition, m5C in tRNA was modified with NSUN2. The reduced size of the frontal lobe in *Nsun2*-KO mouse embryos indicates its involvement in neurodevelopment.[38] Although it is becoming clear that certain RNA modifications are involved in development, this understanding remains fragmented. The behavioral and physiological functions of nearly 300 RNA modifications during development remain unknown. Therefore, this study explored the important RNA modifications during post-fertilization mouse development and performed functional analyses using RNA modification enzymes.

RESULTS

The behavior of the RNA modification mcm5U was distinctive during the mouse developmental process

To explore RNA modifications related to post-fertilization mouse development, total RNA was extracted from MII oocytes, early embryos (pronuclear stage/2-cell stage/morula/blastocyst), embryos (E10.5, 13.5, 16.5, and 19.5), and post-natal day (P)0 individuals (Figure 1A; Table S1).

There have been no reports on the RNA species profiles during mouse development. Gel electrophoresis was used to classify the samples into three categories based on the detection peaks, 28S rRNA, 18S rRNA, and small RNA (Figure S1), to confirm the RNA species profile of the total RNA extracted at each stage. The results demonstrated a high proportion of small RNA in MII oocytes and pronuclear and 2-cell stages, with no significant changes in the RNA species profile from the morula stage onwards (Figure 1B). We examined the electrophoretic profiles of small RNAs and observed a few changes in the microRNA ratio; however, no significant changes were observed in the overall waveform (Figure S2; Table S4).

RNA modification analysis was performed. Our laboratory protocol detected 28 subtypes during mouse development[39] (Table S2). We identified three major clusters: the first cluster includes mcm5U and pseudouridine (Ψ), the second m6A, N6, N6-dimethyladenosine (m6,6A), and 2′-*O*-methyladenosine (Am), and the third cluster included other modifications. We focused on mcm5U, which exhibited characteristic variation among the three clusters.

Although many RNA modifications exhibited changes corresponding to alterations in the RNA species profile, mcm5U expression increased during the 2-cell stage and late fetal development from E13.5, in contrast to the decreasing trend observed for other RNA modifications (Figure 1C). Consequently, considering the potential relevance of mcm5U in the developmental process, this analysis shifted focus to modifying mcm5U. AlkB homolog 8 (ALKBH8), an enzyme involved in mcm5U modification, catalyzes the methylation of 5-carboxymethyluridine (cm5U) to mcm5U[40] (Figure S3). ALKBH8 is responsible for the autosomal recessive intellectual developmental disorder MRT71 in humans. Human ALKBH8 loss-of-function mutations are associated with global developmental delay.[41] Therefore, we hypothesized that mcm5U modification by ALKBH8 may be related to its development.

To examine *Alkbh8* changes during mouse development, mRNA expression levels were assessed using qPCR. *Alkbh8* gene expression and mcm5U levels increased during the fetal period, with the rise in *Alkbh8* starting specifically at E13.5 (Figures 1D and S4A). We conducted a microarray analysis of the modification enzymes involved in the adjacent modifications of mcm5U (Figure S4B). Although a few exhibited trends similar to mcm5U, we considered ALKBH8, which directly influences mcm5U generation, a key factor. Consequently, we considered the possibility that mcm5U modification through ALKBH8 may occur during the fetal period.

A

Stage	Observed				Expected				*Chi*-squared test P-value
	N	Alkbh8			*N*	Alkbh8			
		WT	HKO	KO		WT	HKO	KO	
E10.5	30	5 (16.7%)	17 (56.7%)	8 (26.7%)	32	8 (25%)	16 (50%)	8 (25%)	0.7194
E13.5	98	24 (24.5%)	50 (51.0%)	24 (24.5%)	100	25 (25%)	50 (50%)	25 (25%)	0.9897
E19.5	79	29 (36.7%)	37 (46.8%)	13 (16.5%)	80	20 (25%)	40 (50%)	20 (25%)	0.197
P0	79	21 (26.6%)	49 (62.0%)	9 (11.4%)	80	20 (25%)	40 (50%)	20 (25%)	0.078
4wks	87	32 (36.8%)	48 (55.2%)	7 (8.0%)	88	22 (25%)	44 (50%)	22 (25%)	0.0075 **

B

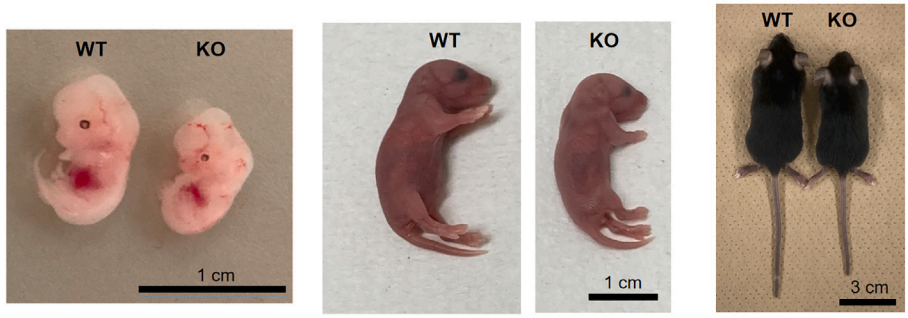

C

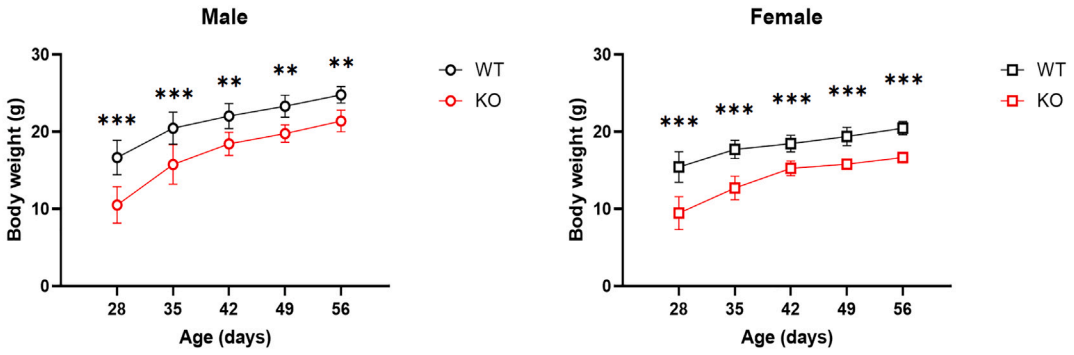

D

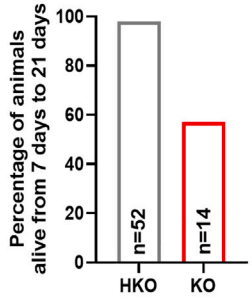

E

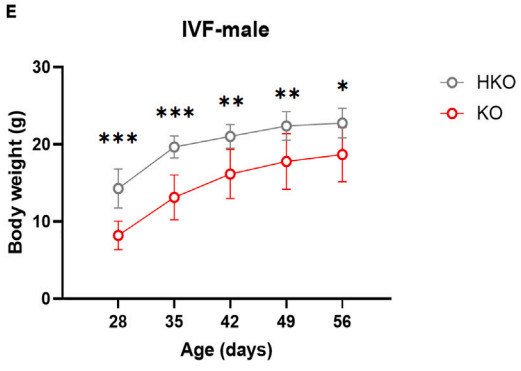

Figure 2. In *Alkbh8*-KO mice, developmental abnormalities were observed

(A) Genotype ratios of offspring from *Alkbh8*-HKO mice crosses at each gestational week or each postpartum week. Each number represents the number of offspring, and the numerical values in parentheses indicate the genotype ratio relative to the total number of offspring. The statistical analysis was conducted using the chi-squared test to compare the observed and expected numbers of mice at each time point (**$p < 0.01$).

(B) Representative photographs of individuals from the offspring of *Alkbh8*-HKO mice crosses (left: E13.5, center: P0, right: P28). A scale bar is included in the photograph (E13.5 and P0: 1 cm; P28: 3 cm).

(C) Post-weaning weight trajectory from 28 to 56 days of age of offspring from *Alkbh8*-HKO mice crosses. (left: male WT $n = 6$, KO $n = 7$; right: female WT $n = 6$, KO $n = 5$) Data are represented as mean ± SD, **$p < 0.01$, ***$p < 0.001$, two-way repeated measures ANOVA followed by Šídák's multiple comparisons test.

(D) Number of offspring for each genotype at P7 and survival rates until P21 obtained by IVF-ET using sperm from *Alkbh8*-KO mice and MII oocytes from *Alkbh8*-HKO mice, followed by transplantation into 16 surrogate ICR mice; n represents the number of offspring at seven days of age, and the bar graph illustrates the survival rate between seven and 21 days of age.

(E) Post-weaning weight trajectories from 28 to 56 days of age of offspring obtained through IVF-ET (male HKO, $n = 11$; KO, $n = 4$). Data are represented as mean ± SD, *$p < 0.05$, **$p < 0.01$, ***$p < 0.001$, two-way repeated measures ANOVA followed by Šídák's multiple comparisons test.

In *Alkbh8*-KO mice, developmental abnormalities were observed

We performed phenotypic analysis using *Alkbh8*-KO mice generated in our laboratory[42] to perform a functional analysis of mcm5U, whose relevance to development is unknown, and the modifying enzyme ALKBH8.

To investigate the effects on development, we examined the genotype ratios of the offspring from mating *Alkbh8*-heterozygous knockout (HKO) mice at E10.5, E13.5, E19.5, P0, and P28 post-weaning (Table S3). The results showed that, up to E13.5, the ratio of wild-type (WT):*Alkbh8*-HKO:*Alkbh8*-homozygous KO was approximately 25:50:25, adhering to Mendel's law of 1:2:1. However, after E13.5, the *Alkbh8*-KO mice ratio showed a decreasing trend and was significantly lower at P28 (Figure 2A). Additionally, observations of *Alkbh8*-KO mice at each fetal age revealed a decrease in body length in *Alkbh8*-KO mice compared to WT mice starting at E13.5, which persisted at P0 and P28 (Figure 2B). Monitoring of post-weaning weight revealed that *Alkbh8*-KO mice exhibited lower body weights than WT mice up to P56 (Figure 2C). Conversely, investigating genotype ratios in the offspring obtained by crossing *Alkbh8*-HKO mice with B6D2F1 mice and monitoring the weight trends revealed a weakened phenotype (Figures S5A and S5B).

We used an *in vitro* fertilization-embryo transfer (IVF-ET) method to determine whether the offspring mortality was related to the offspring or the mother. Fertilization was performed using sperm from *Alkbh8*-KO males and MII oocytes from *Alkbh8*-HKO females, followed by embryo transfer into the uteri of ICR WT females. This method allowed for efficient acquisition of offspring and facilitated analysis, excluding the influence of foster parents. Using IVF-ET, we analyzed the genotype ratios of the offspring obtained from 16 ICR surrogate mothers. At P7, there were 52 *Alkbh8*-HKO mice and 14 *Alkbh8*-KO mice, deviating from the expected 1:1 ratio according to Mendel's law, with significantly fewer *Alkbh8*-KO mice. Mortality occurred in *Alkbh8*-KO mice from P7 to P21, most of which were *Alkbh8*-KO mice (Figure 2D). Examination of post-weaning weight trends revealed that *Alkbh8*-KO mice were underweight up to P56, similar to the natural mating scenario (Figure 2E).

Consequently, *Alkbh8*-KO mice showed reduced survival rates from E13.5 before weaning, and those that survived were smaller. The function of ALKBH8 in the fetus is considered important and independent of maternal influence.

In *Alkbh8*-KO mice, the balance of tRNA in the cytoplasm and mitochondria was altered

Mcm5U is a modified base with a methoxycarbonylmethyl group at the 5th position of the uracil (Figure S3), at the wobble position of the 34 anticodon loop in tRNA. In human cells, ALKBH8 targets $tRNA^{Arg}$(UCU), $tRNA^{Glu}$(UUC), $tRNA^{SeC}$(UCA), $tRNA^{Gly}$(UCC), and $tRNA^{Lys}$(UUU).[43,44] However, its effect on other tRNAs in living organisms remains unclear. We focused on E13.5, when body length reduction begins, and analyzed the effect of tRNA balance in *Alkbh8*-KO mice.

We analyzed RNA modification by fractionating RNA extracted from E13.5 WT and *Alkbh8*-KO whole embryos into large RNA (containing rRNA; ≥200 nucleotides) and small RNA (containing abundant tRNA; <200 nucleotides). The results confirmed that, as previously reported, cm5U was detected in small RNA fractions of *Alkbh8*-KO mice[40]; cm5U decreased in *Alkbh8*-KO mice compared to WT mice, indicating a loss of modification function from cm5U to mcm5U in *Alkbh8*-KO mice (Figures 3A) and S6; Table S5). Similar results were observed in adult *Alkbh8*-KO mice, but the degree of decrease in mcm5U expression varied among tissues (Figure S7).

We comprehensively analyzed tRNA using sequencing (tRNA-seq) to investigate the effects of tRNA species in mice. In small RNA extracted from embryos at E13.5, 171 tRNAs were detected; 76 tRNAs increased, and 11 tRNAs decreased in *Alkbh8*-KO compared to WT (Figures S8 and S9; Table S6).

Among the tRNAs with significant and marked changes (top-10 upregulated and downregulated tRNAs), we confirmed an increase in tRNA-Lys-TTT-2-1, which has been reported to be a target of ALKBH8. In contrast, we observed significant changes in the expression of several tRNAs. The tRNAs that exhibited dramatic changes were primarily mitotRNAs (Figure 3B).

When comparing *Alkbh8*-WT and KO mice in terms of counts per million for each tRNA isoacceptor family, we observed an increasing trend in tRNA-Glu-TTC and tRNA-Arg-TCT, as previously reported (Figure 3C). However, changes in tRNA-Gly-TCC, tRNA-SeC-TCA, and tRNA-Lys-TTT were minimal (Figure S10).

In contrast, tRNAs with uracil at the anticodon wobble position were particularly prominent in mitotRNAs, especially mitotRNA-Glu-TTC (Figure 3D). In Alkbh8-KO mice, the action on cytoplasmic tRNA and the potential to alter the mitotRNA balance have been suggested.

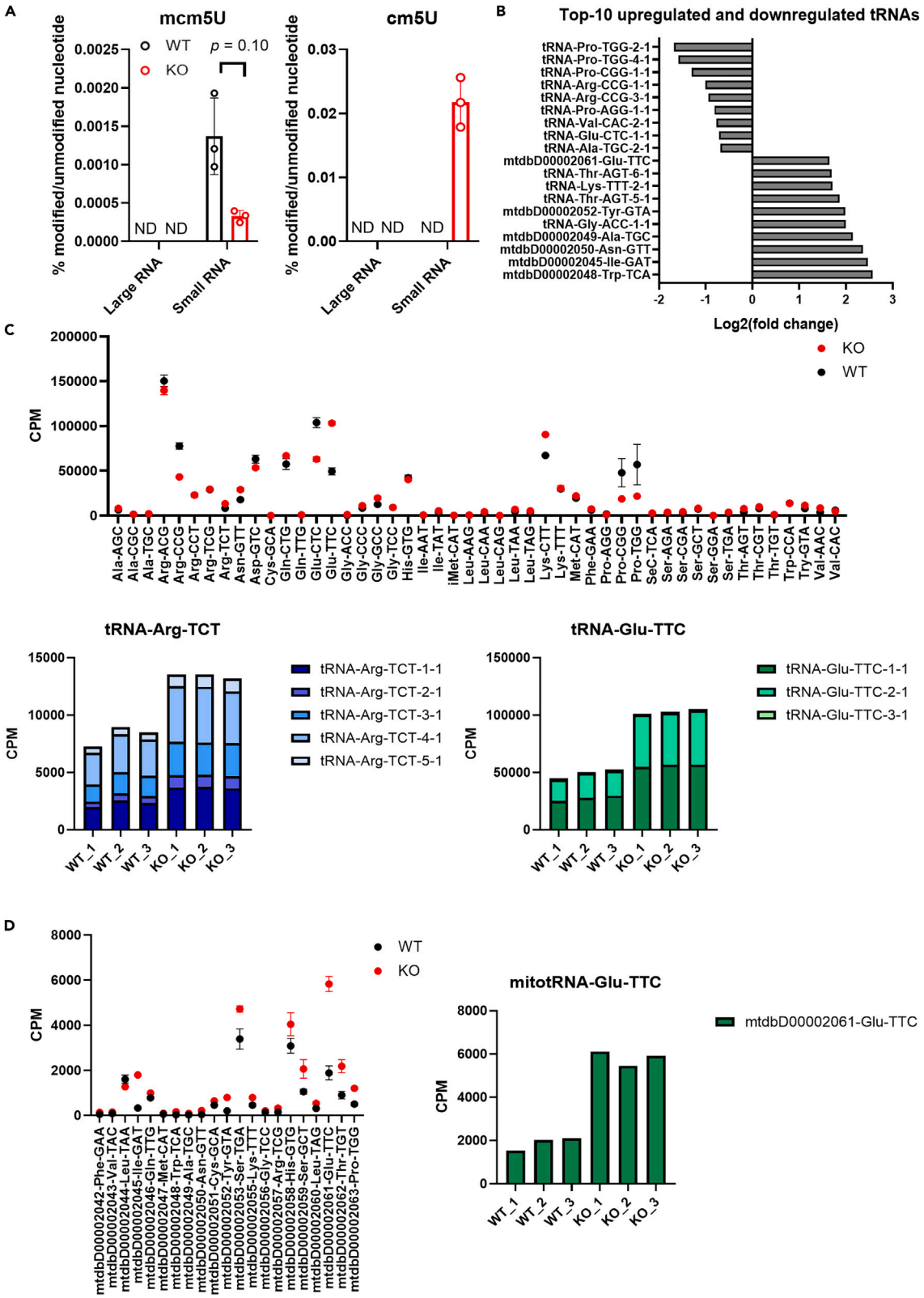
A
mcm5U
% modified/unmodified nucleotide
WT
KO
p = 0.10
ND ND
Large RNA
Small RNA
cm5U
ND ND ND
B
Top-10 upregulated and downregulated tRNAs
tRNA-Pro-TGG-2-1
tRNA-Pro-TGG-4-1
tRNA-Pro-CGG-1-1
tRNA-Arg-CCG-1-1
tRNA-Arg-CCG-3-1
tRNA-Pro-AGG-1-1
tRNA-Val-CAC-2-1
tRNA-Glu-CTC-1-1
tRNA-Ala-TGC-2-1
mtdbD00002061-Glu-TTC
tRNA-Thr-AGT-6-1
tRNA-Lys-TTT-2-1
tRNA-Thr-AGT-5-1
mtdbD00002052-Tyr-GTA
tRNA-Gly-ACC-1-1
mtdbD00002049-Ala-TGC
mtdbD00002050-Asn-GTT
mtdbD00002045-Ile-GAT
mtdbD00002048-Trp-TCA
Log2(fold change)
C
CPM
KO
WT
tRNA-Arg-TCT
tRNA-Arg-TCT-1-1
tRNA-Arg-TCT-2-1
tRNA-Arg-TCT-3-1
tRNA-Arg-TCT-4-1
tRNA-Arg-TCT-5-1
tRNA-Glu-TTC
tRNA-Glu-TTC-1-1
tRNA-Glu-TTC-2-1
tRNA-Glu-TTC-3-1
WT_1
WT_2
WT_3
KO_1
KO_2
KO_3
D
mitotRNA-Glu-TTC
mtdbD00002061-Glu-TTC

Figure 3. In *Alkbh8*-KO mice, the balance of tRNA in the mitochondria was altered

(A) cm5U and mcm5U levels in large/small RNA extracted from WT and *Alkbh8*-KO E13.5 embryos (WT $n = 3$, KO $n = 3$). Data are mean ± SD of three embryos. The statistical analysis was conducted using the Mann-Whitney U test.

(B) The expression levels (log2 fold change) of top-10 upregulated and downregulated proteins in *Alkbh8*-KO E13.5 embryos compared to WT (false discovery rate = 0.2, S0 = 0.1 regulated using the Perseus software).

(C) Graphs showing detected total tRNA isoacceptor (top), tRNA-Glu-TTC (lower left), and tRNA-Arg-TCT (lower right) reads per million in WT and *Alkbh8*-KO E13.5 embryos. Data are represented as mean ± SD of three embryos (black: WT, red: *Alkbh8*-KO).

(D) Graphs showing detected total mitotRNA (left) and mitotRNA-Glu-TTC (right) reads per million in WT and *Alkbh8*-KO E13.5 embryos. Data are represented as mean ± SD of three embryos (black: WT, red: *Alkbh8*-KO).

In *Alkbh8*-KO mice, a decrease in proteins associated with erythroid linage cells and protoporphyrin metabolism was observed

We examined the protein translation capacity of tRNA to investigate the physiological functions induced by changes in both tRNA modification and tRNA balance observed in *Alkbh8*-KO mice. Luciferase activity was evaluated using an *in vitro* translation system containing luciferase RNA and small RNA extracted from E13.5 WT and *Alkbh8*-KO embryos, along with amino acids and translation factors. The results demonstrated a significant decrease in protein translation efficiency in the *Alkbh8*-KO compared to that in WT mice (Figure 4A).

Using quantitative mass spectrometry, we identified nearly 6,527 proteins and conducted a proteomic analysis to confirm changes in protein content in *Alkbh8*-KO mice. Comparative proteomics of E13.5 whole embryo samples from *Alkbh8* WT and KO mice revealed increased 21 proteins and a decreased 111 proteins (Figures 4B and S11; Table S7). Enrichment Analysis of the 111 downregulated proteins suggested potential associations between protoporphyrin metabolism (Figure 4C), erythrocyte-like cells, and erythroid precursors (Figures 4D and S12). Specific factors, such as carcinoembryonic antigen-related cell adhesion molecule 1 (CEACAM1), 5′-aminolevulinate synthase 2 (ALAS2), ferrochelatase (FECH), pyruvate kinase L/R (PKLR), alpha 2-HS glycoprotein (AHSG), uroporphyrinogen III synthase (UROS), pyridoxamine 5′-phosphate oxidase (PNPO), and GATA binding protein 1 (GATA1), were implicated in these processes (Figure 4E), indicating a potential role of ALKBH8 in erythroid linage cells and protoporphyrin metabolism, linking tRNA modifications to these physiological pathways.

In *Alkbh8*-KO mice with mcm5U modification enzyme deficiency, abnormalities in erythroid differentiation were observed

Given the decrease in erythrocyte-related proteins in *Alkbh8*-KO mice with mcm5U deficiency, we focused on the erythroid differentiation of *Alkbh8*-KO mouse embryos. In mouse embryos, erythropoiesis around E13.5 mainly occurs in the liver.[45] To precisely define erythroid precursors in the fetal liver, flow cytometry was performed using the red blood cell surface markers CD71 and Ter119 (Figure S13). The fetal liver can exist in four stages (S1, S2, S3, and S4), representing distinct erythroid differentiation. In previous studies, megakaryocyte-erythroid progenitor and colony-forming unit erythroid were identified as the main components of state 1 (S1), with subsequent progression through S2, S3, and S4[46]. The results demonstrated a significant increase in S2 erythroid precursors and a decrease in differentiated erythroid cells in S3 in *Alkbh8*-KO mice compared to WT mice (Figure 5A). Pathological analysis of the E13.5 liver in *Alkbh8*-KO mice revealed abnormalities in erythroblasts and megakaryocytes (Figure 5B). Compared to WT cells, erythroblasts exhibited larger and smaller sizes, whereas megakaryocytes showed immature and smaller cells, non-segmented mononuclear cells, and cells with exposed nuclei (Figure 5C). Similar trends of decreased red blood cell and hemoglobin counts, and increased mean corpuscular volume and mean platelet volume, were observed in adult *Alkbh8*-KO mice (Figure S14). Evaluation of hematopoietic differentiation capacity through colony-forming unit (CFU) assays using E13.5 revealed that the burst-forming unit-erythroid (BFU-E) decreased. In contrast, the colony-forming units granulocyte-erythroid-macrophage-megakaryocyte (CFU-GEMM) and CFU granulocyte-monocyte (CFU-GM) remained unchanged (Figure 5D). Therefore, *Alkbh8* deficiency in mice led to abnormalities in the differentiation of erythroid precursors.

DISCUSSION

As mentioned in the Introduction, there are over 300 types of RNA modifications, a few of which are presumed to be controlled reversibly or stepwise by intracellular enzymes.[2] Modified RNA subjected to modifications changes its higher-order structure and binds to RNA-binding proteins, leading to alterations in RNA stability, localization, and target specificity, ultimately indirectly controlling protein translation. Abnormalities in RNA modifications have been reported as causative factors of diseases such as cancer, attracting significant attention.[14–21] The role of RNA modifications in development has been increasingly elucidated in recent years,[35–38] suggesting their involvement in developmental processes.

Given these considerations, we analyzed the variations in RNA modifications during the development and performed functional analysis of RNA modification enzymes. First, we analyzed the RNA species profiles during post-fertilization mouse development (pronuclear, 2-cell, morula, blastocyst, E10.5, E13.5, E16.5, E19.5, and P0). MII oocytes at the pronuclear and 2-cell stages exhibited many small RNAs, with no significant changes observed after the morula stage.

From the gel electrophoresis results of small RNA, it can be observed that the peaks of 5S rRNA and 5.8S rRNA were small during the early stages of development, especially in the pronuclear and 2-cell stages, and became larger from the morula stage onwards.

Considering previous reports suggesting that the transcription of rRNA genes begins at the end of the 2-cell stage,[47] we believe our results are consistent with this finding. Furthermore, in mice, the transition from the oocyte to the 2-cell stage involves a maternal-zygotic transition,

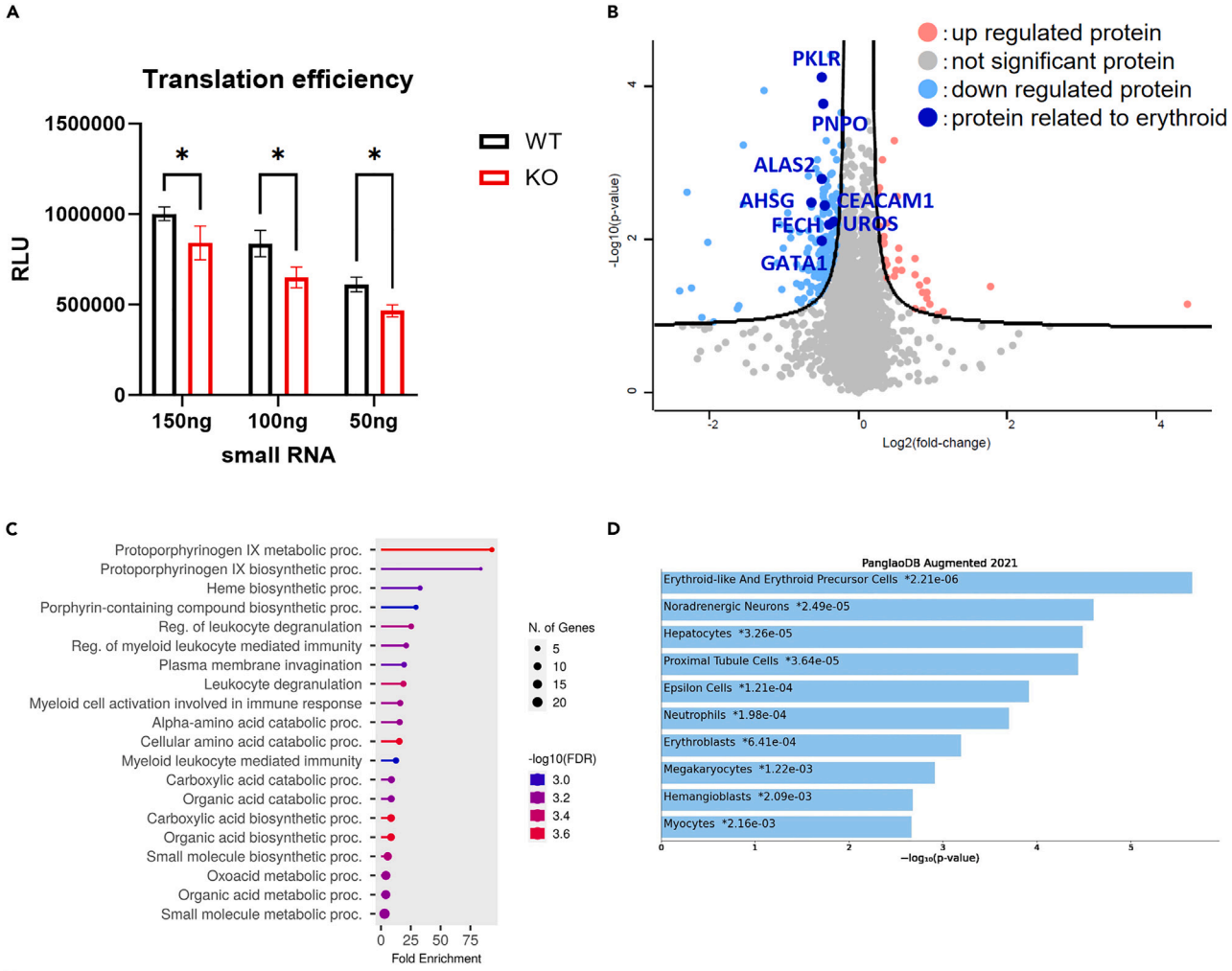

E

Table of top 10 significant p-values and q-values for PanglaoDB Augmented 2021

term	p-value	q-value	overlap_genes
Erythroid-like And Erythroid Precursor Cells	0.000002	0.00029	[CEACAM1, ALAS2, FECH, PKLR, AHSG, UROS, PNPO, GATA1]
Noradrenergic Neurons	0.000025	0.001193	[AGXT2, AHSG, APOH, PAH, GC, OTC]
Hepatocytes	0.000033	0.001193	[AGXT2, AHSG, APOH, PAH, EPPK1, GC, KNG1, OTC]
Proximal Tubule Cells	0.000036	0.001193	[AGXT2, APOH, PAH, FAH, GC, KNG1, OTC]
Epsilon Cells	0.000121	0.00317	[AGXT2, APOH, PAH, GC, AGT, OTC]
Neutrophils	0.000198	0.004319	[CEACAM1, PSTPIP1, ITGAM, ITGB2, PRTN3, MPO]
Erythroblasts	0.000641	0.011996	[ALAS2, RAC2, MPO, GATA1, FERMT3]
Megakaryocytes	0.001216	0.01992	[PSTPIP1, ITGAM, ITGB2, GATA1, FERMT3]
Hemangioblasts	0.002095	0.028347	[ALAS2, SMIM1, GATA1, FERMT3]
Myocytes	0.002164	0.028347	[MYLPF, TNNT3, CASQ2, TNNI2, LDB3]

Figure 4. In *Alkbh8*-KO mice, a decrease in proteins associated with erythroid lineage cells and protoporphyrin metabolism was observed

(A) Protein translation efficiency assessment using small RNA extracted from WT and *Alkbh8*-KO E13.5 embryos at 50, 100, and 150 ng concentrations. The Mann-Whitney U test represents data as mean ± SD of six embryos, $*p < 0.05$.

Figure 4. *Continued*

(B) The volcano plot of proteome analysis of proteins extracted from *Alkbh8*-KO E13.5 embryos compared to WT. Proteins were graphed by log2 (fold change) and −log(*p* value) using a false discovery rate of 0.2 and an S0 of 0.1 regulated using the Perseus software (red, significantly up; blue, significantly down; and highlighted in blue, protein related to erythroid lineage cells). Data are represented as mean of two or three embryos (WT $n = 2$, KO $n = 3$, littermate).

(C) Enrichment analysis of the 111 proteins that significantly decreased in *Alkbh8*-KO E13.5 embryos compared to WT using ShinyGO, referring to gene ontology biological processes.

(D) Enrichment analysis of the 111 proteins that significantly decreased in *Alkbh8*-KO E13.5 embryos compared to WT using Enrichr, referring to PanglaoDB.

(E) The top-10 factors identified in the enrichment analysis of the 111 proteins significantly decreased in *Alkbh8*-KO E13.5 embryos compared to WT using Enrichr, referring to PanglaoDB.

during which maternal factors are degraded and zygote-derived proteins are synthesized. While previous studies have confirmed the scarcity of long RNAs during the 2-cell stage,[48] the dynamic changes in RNA profiles at each developmental stage provide promising insights.

RNA analysis revealed significant changes in many RNA modifications, with the behavior of mcm5U distinct from that of other RNA modifications. It increased during the 2-cell stage and late fetal development from E10.5. Although the analysis in this study was limited to total RNA because of the constraints on the amount of RNA extracted from early embryos, a more detailed change could be revealed by analyzing individual RNA species, such as mRNA and tRNA.

Increased expression of *Alkbh8*, which encodes a mcm5U modification enzyme, was observed at E13.5. However, caution is required as there are stages in which *Alkbh8* and mcm5U expressions are not perfectly correlated. Specifically, while mcm5U increased during the 2-cell stage, there was no increase in *Alkbh8* mRNA. This discrepancy may be explained by changes in ALKBH8 protein levels. It has been speculated that other mcm5U modification enzymes may influence this relationship. For example, the enzymes responsible for the conversion of U to cm5U are the ELP2–6, and those responsible for the conversion of mcm5U to mcm5s2U are the cytosolic thiouridylase subunit (CTU)1 and CTU2.[49]

This is based on the microarray data observation that *Ctu1* and *Ctu2* show a temporary decrease during the 2-cell stage, suggesting transient inhibition of the conversion to mcm5s2U, which could potentially lead to the observed increase in mcm5U.

Phenotypic analysis was conducted using *Alkbh8*-KO mice to perform a functional analysis of mcm5U and its modifying enzyme, ALKBH8, whose developmental relevance is unknown. The results revealed that *Alkbh8*-KO mice had a lower survival rate from E13.5, even without parental care, and those that survived were born smaller, suggesting a potential role for ALKBH8 in early development. Deaths occurred between P0 and P28. The cause of these deaths has not been identified, but it is speculated that they may be attributed to low birth weight, resulting in a loss of competition for survival or potential cannibalism in the mother mouse. Previous studies suggested that *Alkbh8*-KO mice do not exhibit developmental effects.[37,50,51]

While a previous study reported a dramatic decrease in mcm5U in total RNA from the adult mouse liver, testis, and brain,[37] we observed a decrease in mcm5U in small RNA from 13 organs. The content of mcm5U varied among organs in adult mice, and the reduction rate of mcm5U due to *Alkbh8*-KO differed (with lower reduction rates observed in the brain and skeletal muscle). Although direct comparisons with adult mice may not be straightforward, we speculate that the 10%–20% residual mcm5U levels we demonstrated in whole fetal tissues might represent tissues where mcm5U reduction was not detected.

Our murine model was created by acquiring the genome of a bacterial artificial chromosome clone and integrating it into 129 mouse ES-D3 cells, followed by introduction into C57BL/6 blastocysts. Initially, no discernible phenotype was observed in the mice, but abnormalities in the number of offspring were noticed during the backcrossing process. Examination of the genotype ratio of offspring obtained from crosses with B6D2F1 *Alkbh8*-HKO mice and confirmation of the weight trajectory revealed a diminished phenotype.

This research result, discovered over several years of repeated backcrossing to establish a congenic strain, aligns with the developmental disorders observed in familial *ALKBH8* deficiency in humans, particularly in regions such as Saudi Arabia, Egypt, and Yemen.[52]

Continuing with the observation of reduced body length at E13.5, we analyzed the impact of mcm5U-modified RNA on ALKBH8. Analysis of small RNA extracted from the entire body of *Alkbh8*-KO mice at E13.5 revealed changes in the tRNA balance associated with a reduction in mcm5U modification. In human cells, ALKBH8 targets mcm5U modifications in specific tRNAs, including $tRNA^{Arg}$(UCU), $tRNA^{Glu}$(UUC), $tRNA^{SeC}$(UCA), $tRNA^{Gly}$(UCC), and $tRNA^{Lys}$(UUU).[43,44] The current study confirmed the potential targeting of $tRNA^{Arg}$(UCU) and $tRNA^{Glu}$(UUC) in *Alkbh8*-KO mice, consistent with previous reports; it discovered a potential contribution to changes in mitotRNA balance.

The detailed mechanism of tRNA expression variation in *Alkbh8*-KO mice and the role of ALKBH8 in controlling mcm5U modification in mtRNA were not clarified in this study and require further investigation. Although no specific reports have addressed ALKBH8's modulation of mitotRNAs, a previous study implied that *Alkbh8* deficiency correlates with cellular senescence and mitochondrial reprogramming.[53] Considering that mitochondrial dysfunction may be linked to the alterations in the mitotRNA equilibrium observed in our investigation, it is reasonable to explore the potential role of ALKBH8 in regulating mitotRNAs. Assessing the mitochondrial localization of the ALKBH8 protein and evaluating mitochondrial function could open avenues for further investigation in this domain.

Alterations in tRNAs lacking uridine at the anticodon were noted in *Alkbh8*-KO mice. To our knowledge, the mechanisms governing tRNAs lacking uridine in the anticodon have not yet been elucidated. In terms of the discussion, two conjectures can be considered, which are discussed in the following.

One possibility is that modifications occurring in regions of the tRNA body other than the anticodon contributed to these variations. Certain tRNA-modifying enzymes demonstrate dual specificity for tRNA species and modification sites, suggesting that ALKBH8 is an exception.[54,55] For instance, NSUN2 has been reported to introduce m5C at the C34 position of tRNA and positions 48, 49, and 50, depending on the tRNA.[54,55] ALKBH8 bound to multiple tRNAs, including those lacking mcm5U, as evidenced by high-throughput sequencing of RNA

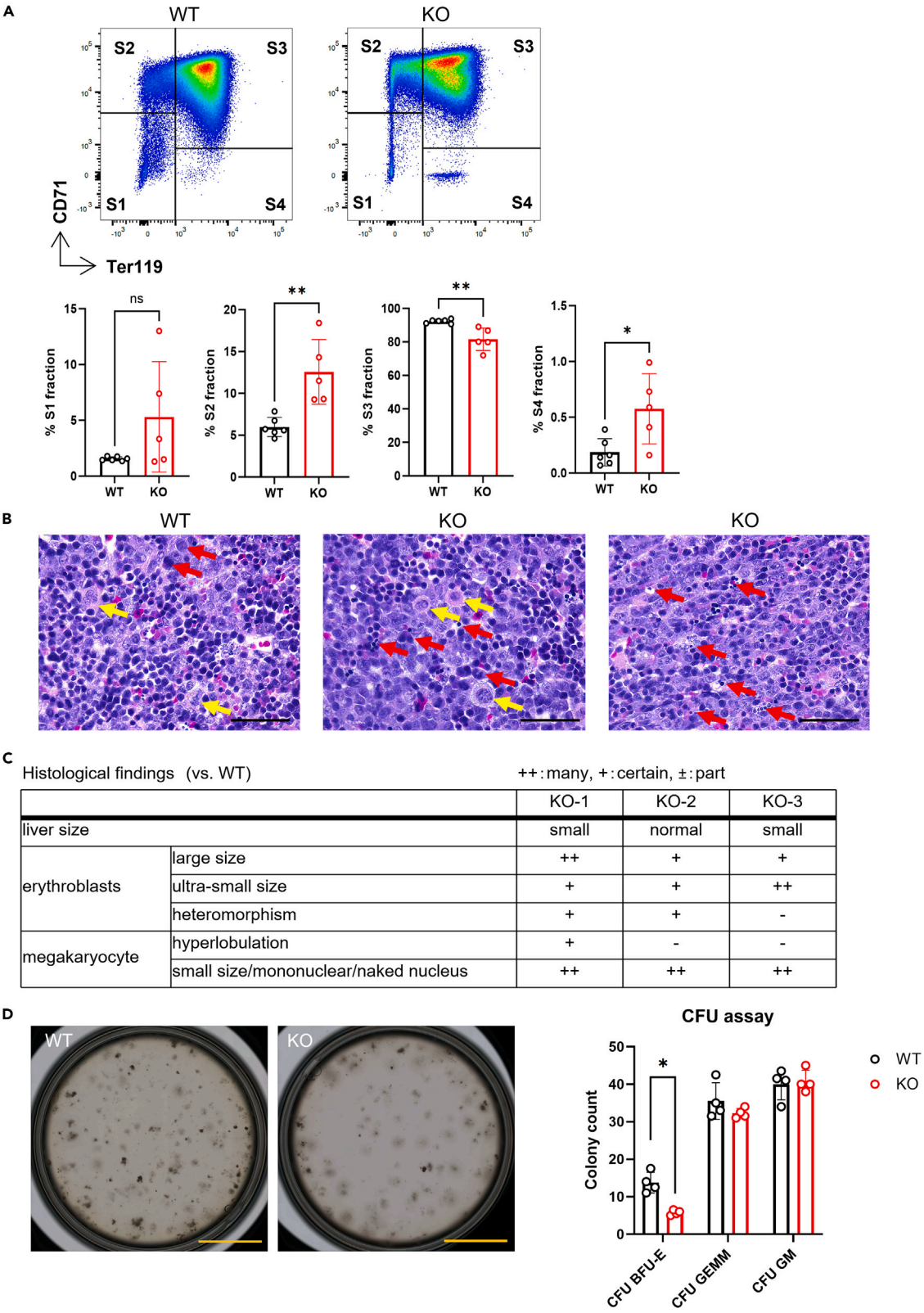

C

Histological findings (vs. WT)

++: many, +: certain, ±: part

		KO-1	KO-2	KO-3
liver size		small	normal	small
erythroblasts	large size	++	+	+
	ultra-small size	+	+	++
	heteromorphism	+	+	-
megakaryocyte	hyperlobulation	+	-	-
	small size/mononuclear/naked nucleus	++	++	++

Figure 5. In *Alkbh8*-KO mice with mcm5U modification enzyme deficiency, abnormalities in erythroid differentiation were observed

(A) Analysis of erythrocyte differentiation in the E13.5 liver using flow cytometry. Top: representative dot plots of CD71/Ter119 in the liver of WT and *Alkbh8*-KO E13.5 embryos. Bottom: population analysis at each state (S1:CD71^{low}/Ter119^{low}, S2:CD71^{high}/Ter119^{low}, S3:CD71^{high}/Ter119^{high}, and S4:CD71^{low}/Ter119^{high}). Data are mean ± SD, *$p < 0.05$, **$p < 0.01$ by Mann-Whitney U test. WT: six mice, KO: five mice. ns, not significant.

(B) Representative photomicrographs of hematoxylin and eosin staining in the liver of WT and *Alkbh8*-KO E13.5 embryos. Red: erythrocyte; yellow: megakaryocyte; WT: three mice; KO: three mice. Scale bar, 50 μm.

(C) Pathohistological analysis results of the liver in *Alkbh8*-KO E13.5 embryos compared to WT.

(D) CFU assay using liver cells from WT and *Alkbh8*-KO E13.5 embryos (WT: four mice KO: four mice). Left: representative photographs of liver cell cultures from WT and *Alkbh8*-KO E13.5 embryos on day 10. Right: number of BFU-E, CFU-GEMM, and CFU-GM colonies. Scale bar, 1 cm.

isolated by cross-linking immunoprecipitation and RNA immunoprecipitation sequencing (RIP-seq). This implies the potential of ALKBH8 to regulate the tRNA balance independent of mcm5U. Further investigations are required to provide additional insights into this aspect.[44]

Alternatively, complementary fluctuations in other tRNAs may occur in response to fluctuations in tRNAs containing uridine at the anticodon. Considering reports suggesting the importance of tRNA^{Phe}(GAA) and its gene tRNA-Phe-1-1 in neural function and partial compensation through increased expression of other tRNAs leading to mistranslation, abnormalities in mcm5U modification in tRNA have been suggested to be associated with changes in tRNA balance.[56]

By investigating the impact of tRNA balance changes observed in *Alkbh8*-KO mice on protein translation, we observed a decrease in the protein translation efficiency of tRNAs derived from *Alkbh8*-KO mice. A reduction in proteins primarily involved in erythrocyte differentiation and protoporphyrin metabolism was observed. *In vivo*, protoporphyrin metabolism primarily refers to the pathway by which protoporphyrin generated from 5-aminolevulinic acid in the mitochondria binds iron to produce heme.[57] The observed imbalance in mitotRNA suggests a potential role for this metabolic pathway. Because heme is essential for hemoglobin synthesis in erythrocytes, the suggested association with abnormalities in erythroblast differentiation may have contributed to the observed phenotypes.

In previous studies, it was reported that, in the livers of *Alkbh8* mutant mice, the inhibition of 5-methoxycarbonylmethylation of tRNA^{SeC}(UCA) resulted in a decrease in selenoprotein expression, demonstrating the role of position 34 uridine modification in protein translation.[40] However, no changes in the selenoprotein levels were detected in the current study. As this study focused on embryos, it is plausible that the regulation of proteins other than those in the adult liver was prioritized.

While this study did not directly demonstrate a mechanism of direct protein translation control through tRNA modification, the previously reported functions of tRNA modifications such as methylation, including the prevention of frameshifts, stabilization of tRNA, enhancement of codon-anticodon binding, and fluctuating base pair formation, are all crucial in tRNA-mediated protein translation.[58–60] The mcm5U modification in tRNA discovered in this study may similarly enhance protein translation during dynamic changes in the developmental process through one or more of the aforementioned functions.

Finally, evaluation of erythroblast differentiation ability in *Alkbh8*-KO mouse embryos revealed abnormalities in the differentiation of erythroblast precursors, suggesting that developmental abnormalities in Alkbh8 may be due to defects in erythroblast differentiation. The expression of *Alkbh8* was validated using two single-cell analysis databases (Mouse Cell Atlas [https://bis.zju.edu.cn/MCA/] and Tabula Muris [https://tabula-muris.ds.czbiohub.org/]), which revealed its relatively high localization in neurons and red blood cell precursors. Thus, the requirement for RNA modification enzymes during development varies by cell type, with ALKBH8 playing a particularly significant role as a red blood cell precursor.

A slight difference was observed in the peripheral blood of surviving adult mice, but no obvious abnormalities were detected. Since the body weight trajectory in adult mice was the same between the WT and deficient mice, it is unlikely that hematopoietic growth impairment occurs after birth. Therefore, we speculate that the observed effects are specific to the fetal development period.

To determine whether abnormal red blood cell differentiation is associated with mortality, we considered the following: during the fetal period, hematopoiesis occurs in the liver at approximately E14.5 and shifts to the bone marrow from E18.5. The current study confirmed the liver's red blood cell differentiation abnormalities at E13.5. While the tendency for a decrease in *Alkbh8*-KO offspring occurs after E19.5, determining whether this is the immediate cause of death based on the current results alone is inconclusive.

Hypotheses for abnormalities in fetal red blood cell differentiation include insufficient hematopoiesis only in the liver, inadequate hematopoiesis in the bone marrow after E18.5, and inadequate transition of hematopoiesis from the liver to the bone marrow. Additional verification, such as establishing mice with hematopoietic cell-specific deficiencies in various organs, is necessary to elucidate the mechanisms leading to mortality.

In conclusion, our results suggest that ALKBH8 facilitates changes in tRNA balance in conjunction with mcm5U modification in tRNA, modulating the physiological function of protein translation adjustment and specifically influencing erythroblast differentiation.

Over the past five years, research on RNA modifications has advanced globally rapidly, driven by the development of antibodies against modified bases and transcriptome analyses using next-generation sequencing. Progress is expected to continue, leading to a better understanding of the precise location and biological significance of RNA modifications. We hope that our findings contribute to promising avenues in the field of RNA modification research.

Limitations of the study

Firstly, one of the limitations of this study is that a detailed investigation into modifications other than mcm5U during the developmental process has not been conducted. While this thesis does not offer an in-depth analysis, it is conceivable that other RNA modifications may

influence development. For instance, Y, identified in the initial cluster, is ubiquitous across RNA constituents, such as tRNA, rRNA, small nuclear RNA, and small nucleolar RNA, thereby contributing to structural fortification, as documented.[61] Secondary clustering predominantly encompasses mRNA containing m6A derivatives.[2] These modifications are orchestrated by writers (methylation deposition), readers (binding to modified RNA), and erasers (methylation removal), affecting various facets of the mRNA life cycle, including splicing, export, decay, and translation.[62] These modifications may be associated with development. Additionally, N6-isopentenyladenosine (i6A) is another notable RNA modification. Reports have suggested that a human single-nucleotide polymorphism of the i6A modification enzyme tRNA isopentenyltransferase 1 (TRIT1) is associated with microcephaly and seizures due to mitochondrial dysfunction caused by i6A deficiency in mitotRNA, indicating the potential contribution of i6A to normal development and growth.[20,63]

The observed variations in modified nucleosides within total RNA in this study cannot rule out the possibility that these changes were due to variations in tRNA levels. It is well established that the levels of different tRNA species are differentially regulated, for example, in cancer.[64] Additionally, it has been shown in yeast that mcm5U is present in $tRNA^{Gly}$(UCC) and $tRNA^{Arg}$(UCU)[44]; however, the tRNA species in which mcm5U has been identified in mammals remain unknown except $tRNA^{SeC}$(UCA). By investigating modifications in isolated each tRNA such as $tRNA^{Glu}$(UUC) in mammals, including mice, we believe that we can explain the changes during development and the direct mechanisms of tRNA modifications mediated by Alkbh8.

Furthermore, during the initial phase of this study, our investigation was primarily exploratory, focusing on a comprehensive examination of the whole fetal body at E13.5. Considering the changes in erythrocytes and the more pronounced alterations in *Alkbh8*-KO genotype ratios at P28, we consider conducting separate validations for each organ, such as the brain and liver, or tracking changes at different developmental stages, such as later developmental stages and the neonatal period. We believe that this approach yields more accurate and meaningful results.

This study's approach to measuring mcm5U has certain limitations. This study focuses on ALKBH8, a mcm5U modification enzyme, and discusses data from *Alkbh8*-KO mice. ALKBH8 is not responsible for simply turning mcm5U modifications on and off; instead, it involves multiple modifications occurring simultaneously and acting synergistically with multiple modifying enzymes on mcm5U. Considering these factors, it is challenging to clarify the physiological role of each modification at each stage, that is, the physiological role of mcm5U. For example, ALKBH8 regulates mcm5U, mcm5s2U, and 5-methoxycarbonylmethyl-2′-*O*-methyluridine.[40,65] In addition to ALKBH8, CTU2 has been reported as a conversion enzyme for mcm5s2U in yeast and nematodes. Given the reports suggesting that mutations in CTU2 are associated with dysmorphic facies and congenital microcephaly in humans, mcm5s2U may contribute to certain phenotype.[66,67] ALKBH8 does not act on one of the unmodified bases (A, C, G, and U), but rather on the already modified precursor cm5U, which again requires the elongator complex (Elp1–6) for its formation.[49,68] To confirm the specificity of ALKBH8 for mcm5U, experiments involving combinations of multiple mcm5U-related enzymes will likely provide more detailed insights into these regulatory mechanisms. RIP-seq using RNA modification-specific antibodies is a common method for identifying RNA species with altered properties and modifications in RNA modification studies. A more detailed examination will be possible with the development of antibodies against mcm5U or its surrounding RNA modifications.

Our study focuses on the late fetal stages, and, therefore, the effects of Alkbh8 on early embryos have not been sufficiently analyzed. For instance, we have not been able to explain the transient increase in mcm5U during the 2-cell stage, highlighting the need for protein-level analysis. While we currently present data at the mRNA level, it is highly likely that the protein expression level of Alkbh8 in early embryos is low, which poses limitations for existing detection systems. A more comprehensive understanding could be achieved by increasing the number of collected embryos to secure sufficient protein quantities for western blotting or proteome analysis, or by obtaining commercially available Alkbh8 antibodies suitable for immunostaining.

In summary, the analysis of only a single RNA modification or a single modifying enzyme is insufficient on the developmental process of mice. By comprehensively analyzing mcm5U, its surrounding RNA modifications, ALKBH8, and related modifying enzymes, we expect that the interpretation of the physiological significance of RNA modifications will advance.

RESOURCE AVAILABILITY

Lead contact

Further information and requests for resources and reagents should be directed to and will be fulfilled by the lead contact, Hiroaki Hase (hase-h@phs.osaka-u.ac.jp).

Materials availability

This study did not generate new unique reagents.

Data and code availability

- Raw MS data have been deposited at jPOST repository and are publicly available as of the date of publication (jPOST ID: JPST002999). Additionally, tRNA-seq and microarray data analysis have been uploaded to Gene Expression Omnibus (GEO) and are publicly available as of the date of publication. Accession numbers are also listed in the key resources table.
- Any additional information required to reanalyze the data reported in this paper is available from the lead contact upon request.

ACKNOWLEDGMENTS

This research was partially supported by the Research Support Project for Life Science and Drug Discovery (Basis for Supporting Innovative Drug Discovery and Life Science Research [BINDS]) from AMED under grant numbers JP23ama121054 and JP23ama121052. The graphical abstract was created with BioRender.com.

AUTHOR CONTRIBUTIONS

M.N.: conceptualization of the methodology, investigation, data curation, formal analysis, visualization, writing, supervision, and project administration. H.H.: writing – review and editing and supervision Y.Z.: investigation and validation. K.O.: investigation and validation. K.H.: investigation and validation. K.I.: investigation and validation. K.K.: investigation and validation. K.T.: conceptualization, writing – review and editing, supervision, funding acquisition, and project administration.

DECLARATION OF INTERESTS

The authors declare no competing interests.

STAR★METHODS

Detailed methods are provided in the online version of this paper and include the following:

- KEY RESOURCES TABLE
- EXPERIMENTAL MODEL AND STUDY PARTICIPANT DETAILS
  - Animals
  - Embryo culture
- METHOD DETAILS
  - Genotyping
  - *In vitro* fertilization-embryo transfer (IVF-ET)
  - RNA extraction from animal tissues
  - Quantification of RNA nucleosides
  - qPCR
  - Microarray
  - tRNA-seq
  - *In vitro* translation assay
  - Proteome analysis
  - Flow cytometry
  - Pathological analysis
  - Colony-forming unit (CFU) assay
  - Hematology analysis
- QUANTIFICATION AND STATISTICAL ANALYSIS

SUPPLEMENTAL INFORMATION

Supplemental information can be found online at https://doi.org/10.1016/j.isci.2024.110777.

Received: January 22, 2024
Revised: June 19, 2024
Accepted: August 16, 2024
Published: August 22, 2024

REFERENCES

1. Cohn, W.E., and Volkin, E. (1951). Nucleoside-5′-phosphates from Ribonucleic Acid. Nature *167*, 483–484. https://doi.org/10.1038/167483a0.
2. Machnicka, M.A., Milanowska, K., Osman Oglou, O., Purta, E., Kurkowska, M., Olchowik, A., Januszewski, W., Kalinowski, S., Dunin-Horkawicz, S., Rother, K.M., et al. (2013). MODOMICS: a Database of RNA Modification Pathways–2013 Update. Nucleic Acids Res. *41*, D262–D267. https://doi.org/10.1093/nar/gks1007.
3. Björk, G.R., Ericson, J.U., Gustafsson, C.E., Hagervall, T.G., Jönsson, Y.H., and Wikström, P.M. (1987). Transfer RNA Modification. Annu. Rev. Biochem. *56*, 263–287. https://doi.org/10.1146/annurev.bi.56.070187.001403.
4. Dominissini, D., Moshitch-Moshkovitz, S., Schwartz, S., Salmon-Divon, M., Ungar, L., Osenberg, S., Cesarkas, K., Jacob-Hirsch, J., Amariglio, N., Kupiec, M., et al. (2012). Topology of the Human and Mouse m6A RNA Methylomes Revealed by m6A-seq. Nature *485*, 201–206. https://doi.org/10.1038/nature11112.
5. Meyer, K.D., Saletore, Y., Zumbo, P., Elemento, O., Mason, C.E., and Jaffrey, S.R. (2012). Comprehensive Analysis of mRNA Methylation Reveals Enrichment in 3′ UTRs and near Stop Codons. Cell *149*, 1635–1646. https://doi.org/10.1016/j.cell.2012.05.003.
6. Meyer, K.D., Patil, D.P., Zhou, J., Zinoviev, A., Skabkin, M.A., Elemento, O., Pestova, T.V., Qian, S.B., and Jaffrey, S.R. (2015). 5′ UTR m(6) A Promotes Cap-Independent Translation. Cell *163*, 999–1010. https://doi.org/10.1016/j.cell.2015.10.012.
7. Liu, J., Yue, Y., Han, D., Wang, X., Fu, Y., Zhang, L., Jia, G., Yu, M., Lu, Z., Deng, X., et al. (2014). A METTL3-METTL14 Complex Mediates Mammalian nuclear RNA N6-Adenosine Methylation. Nat. Chem. Biol. *10*, 93–95. https://doi.org/10.1038/nchembio.1432.
8. Jia, G., Fu, Y., Zhao, X., Dai, Q., Zheng, G., Yang, Y., Yi, C., Lindahl, T., Pan, T., Yang, Y.G., and He, C. (2011). N6-Methyladenosine in nuclear RNA Is a Major Substrate of the Obesity-Associated FTO. Nat. Chem. Biol. *7*, 885–887. https://doi.org/10.1038/nchembio.687.
9. Aik, W., Scotti, J.S., Choi, H., Gong, L., Demetriades, M., Schofield, C.J., and McDonough, M.A. (2014). Structure of Human RNA N(6)-methyladenine Demethylase ALKBH5 Provides Insights into Its Mechanisms of Nucleic Acid Recognition and Demethylation. Nucleic Acids Res. *42*, 4741–4754. https://doi.org/10.1093/nar/gku085.
10. Wang, X., Lu, Z., Gomez, A., Hon, G.C., Yue, Y., Han, D., Fu, Y., Parisien, M., Dai, Q., Jia, G., et al. (2014). N6-methyladenosine-dependent Regulation of Messenger RNA Stability. Nature *505*, 117–120. https://doi.org/10.1038/nature12730.
11. Wang, X., Zhao, B.S., Roundtree, I.A., Lu, Z., Han, D., Ma, H., Weng, X., Chen, K., Shi, H., and He, C. (2015). N(6)-methyladenosine Modulates Messenger RNA Translation Efficiency. Cell *161*, 1388–1399. https://doi.org/10.1016/j.cell.2015.05.014.
12. Liu, N., Dai, Q., Zheng, G., He, C., Parisien, M., and Pan, T. (2015). N(6)-methyladenosine-dependent RNA Structural Switches Regulate RNA-Protein Interactions. Nature *518*, 560–564. https://doi.org/10.1038/nature14234.
13. Fustin, J.M., Doi, M., Yamaguchi, Y., Hida, H., Nishimura, S., Yoshida, M., Isagawa, T., Morioka, M.S., Kakeya, H., Manabe, I., and Okamura, H. (2013). RNA-Methylation-Dependent RNA Processing Controls the Speed of the Circadian Clock. Cell *155*,

793–806. https://doi.org/10.1016/j.cell.2013.10.026.
14. Lin, S., Choe, J., Du, P., Triboulet, R., and Gregory, R.I. (2016). The m(6)A Methyltransferase METTL3 Promotes Translation in Human Cancer Cells. Mol. Cell *62*, 335–345. https://doi.org/10.1016/j.molcel.2016.03.021.
15. Zhang, C., Samanta, D., Lu, H., Bullen, J.W., Zhang, H., Chen, I., He, X., and Semenza, G.L. (2016). Hypoxia Induces the Breast Cancer Stem Cell Phenotype by HIF-Dependent and ALKBH5-Mediated m(6)A-demethylation of NANOG mRNA. Proc. Natl. Acad. Sci. USA *113*, E2047–E2056. https://doi.org/10.1073/pnas.1602883113.
16. Cui, Q., Shi, H., Ye, P., Li, L., Qu, Q., Sun, G., Sun, G., Lu, Z., Huang, Y., Yang, C.G., et al. (2017). m(6)A RNA Methylation Regulates the Self-Renewal and Tumorigenesis of Glioblastoma Stem Cells. Cell Rep. *18*, 2622–2634. https://doi.org/10.1016/j.celrep.2017.02.059.
17. Li, Z., Weng, H., Su, R., Weng, X., Zuo, Z., Li, C., Huang, H., Nachtergaele, S., Dong, L., Hu, C., et al. (2017). FTO Plays an Oncogenic Role in Acute Myeloid Leukemia as a N(6)-Methyladenosine RNA Demethylase. Cancer Cell *31*, 127–141. https://doi.org/10.1016/j.ccell.2016.11.017.
18. Zhang, S., Zhao, B.S., Zhou, A., Lin, K., Zheng, S., Lu, Z., Chen, Y., Sulman, E.P., Xie, K., Bögler, O., et al. (2017). m(6)A Demethylase ALKBH5 Maintains Tumorigenicity of Glioblastoma Stem-Like Cells by Sustaining FOXM1 Expression and Cell Proliferation Program. Cancer Cell *31*, 591–606.e6. https://doi.org/10.1016/j.ccell.2017.02.013.
19. Kwok, C.T., Marshall, A.D., Rasko, J.E.J., and Wong, J.J.L. (2017). Genetic Alterations of m(6)A Regulators Predict Poorer Survival in Acute Myeloid Leukemia. J. Hematol. Oncol. *10*, 39. https://doi.org/10.1186/s13045-017-0410-6.
20. Suzuki, T. (2021). The Expanding World of tRNA Modifications and Their Disease Relevance. Nat. Rev. Mol. Cell Biol. *22*, 375–392. https://doi.org/10.1038/s41580-021-00342-0.
21. Cui, W., Zhao, D., Jiang, J., Tang, F., Zhang, C., and Duan, C. (2023). tRNA Modifications and Modifying Enzymes in Disease, the Potential Therapeutic Targets. Int. J. Biol. Sci. *19*, 1146–1162. https://doi.org/10.7150/ijbs.80233.
22. Crick, F.H. (1966). Codon–anticodon pairing: the wobble hypothesis. J. Mol. Biol. *19*, 548–555. https://doi.org/10.1016/s0022-2836(66)80022-0.
23. Moustafa, M.E., Carlson, B.A., El-Saadani, M.A., Kryukov, G.V., Sun, Q.A., Harney, J.W., Hill, K.E., Combs, G.F., Feigenbaum, L., Mansur, D.B., et al. (2001). Selective inhibition of selenocysteine tRNA maturation and selenoprotein synthesis in transgenic mice expressing isopentenyladenosine-deficient selenocysteine tRNA. Mol. Cell Biol. *21*, 3840–3852. https://doi.org/10.1128/MCB.21.11.3840-3852.2001.
24. Huang, B., Johansson, M.J.O., and Byström, A.S. (2005). An early step in wobble uridine tRNA modification requires the Elongator complex. RNA (New York, N.Y.) *11*, 424–436. https://doi.org/10.1261/rna.7247705.
25. Johansson, M.J.O., Xu, F., and Byström, A.S. (2018). Elongator-a tRNA modifying complex that promotes efficient translational decoding. Biochim. Biophys. Acta. Gene Regul. Mech. *1861*, 401–408. https://doi.org/10.1016/j.bbagrm.2017.11.006.
26. Krutyhołowa, R., Zakrzewski, K., and Glatt, S. (2019). Charging the code - tRNA modification complexes. Curr. Opin. Struct. Biol. *55*, 138–146. https://doi.org/10.1016/j.sbi.2019.03.014.
27. Chen, Y.T., Hims, M.M., Shetty, R.S., Mull, J., Liu, L., Leyne, M., and Slaugenhaupt, S.A. (2009). Loss of mouse Ikbkap, a subunit of elongator, leads to transcriptional deficits and embryonic lethality that can be rescued by human IKBKAP. Mol. Cell Biol. *29*, 736–744. https://doi.org/10.1128/MCB.01313-08.
28. Nakano, S., Suzuki, T., Kawarada, L., Iwata, H., Asano, K., and Suzuki, T. (2016). NSUN3 methylase initiates 5-formylcytidine biogenesis in human mitochondrial tRNA(Met). Nat. Chem. Biol. *12*, 546–551. https://doi.org/10.1038/nchembio.2099.
29. Haag, S., Sloan, K.E., Ranjan, N., Warda, A.S., Kretschmer, J., Blessing, C., Hübner, B., Seikowski, J., Dennerlein, S., Rehling, P., et al. (2016). NSUN3 and ABH1 modify the wobble position of mt-tRNAMet to expand codon recognition in mitochondrial translation. The EMBO journal *35*, 2104–2119. https://doi.org/10.15252/embj.201694885.
30. Fakruddin, M., Wei, F.Y., Suzuki, T., Asano, K., Kaieda, T., Omori, A., Izumi, R., Fujimura, A., Kaitsuka, T., Miyata, K., et al. (2018). Defective Mitochondrial tRNA Taurine Modification Activates Global Proteostress and Leads to Mitochondrial Disease. Cell Rep. *22*, 482–496. https://doi.org/10.1016/j.celrep.2017.12.051.
31. Väre, V.Y.P., Eruysal, E.R., Narendran, A., Sarachan, K.L., and Agris, P.F. (2017). Chemical and Conformational Diversity of Modified Nucleosides Affects tRNA Structure and Function. Biomolecules *7*, 29. https://doi.org/10.3390/biom7010029.
32. Tuorto, F., Liebers, R., Musch, T., Schaefer, M., Hofmann, S., Kellner, S., Frye, M., Helm, M., Stoecklin, G., and Lyko, F. (2012). RNA Cytosine Methylation by Dnmt2 and NSun2 Promotes tRNA Stability and Protein Synthesis. Nat. Struct. Mol. Biol. *19*, 900–905. https://doi.org/10.1038/nsmb.2357.
33. Schaefer, M., Pollex, T., Hanna, K., Tuorto, F., Meusburger, M., Helm, M., and Lyko, F. (2010). RNA Methylation by Dnmt2 Protects Transfer RNAs against Stress-Induced Cleavage. Genes Dev. *24*, 1590–1595. https://doi.org/10.1101/gad.586710.
34. Blanco, S., Dietmann, S., Flores, J.V., Hussain, S., Kutter, C., Humphreys, P., Lukk, M., Lombard, P., Treps, L., Popis, M., et al. (2014). Aberrant Methylation of tRNAs Links Cellular Stress to Neuro-developmental Disorders. EMBO J. *33*, 2020–2039. https://doi.org/10.15252/embj.201489282.
35. Geula, S., Moshitch-Moshkovitz, S., Dominissini, D., Mansour, A.A., Kol, N., Salmon-Divon, M., Hershkovitz, V., Peer, E., Mor, N., Manor, Y.S., et al. (2015). Stem Cells. m6A mRNA Methylation Facilitates Resolution of Naive Pluripotency Toward Differentiation. Science *347*, 1002–1006. https://doi.org/10.1126/science.1261417.
36. Batista, P.J., Molinie, B., Wang, J., Qu, K., Zhang, J., Li, L., Bouley, D.M., Lujan, E., Haddad, B., Daneshvar, K., et al. (2014). m(6)A RNA Modification Controls Cell Fate Transition in Mammalian Embryonic Stem Cells. Cell Stem Cell *15*, 707–719. https://doi.org/10.1016/j.stem.2014.09.019.
37. Wang, Y., Li, Y., Toth, J.I., Petroski, M.D., Zhang, Z., and Zhao, J.C. (2014). N6-Methyladenosine Modification Destabilizes Developmental Regulators in Embryonic Stem Cells. Nat. Cell Biol. *16*, 191–198. https://doi.org/10.1038/ncb2902.
38. Flores, J.V., Cordero-Espinoza, L., Oeztuerk-Winder, F., Andersson-Rolf, A., Selmi, T., Blanco, S., Tailor, J., Dietmann, S., and Frye, M. (2017). Cytosine-5 RNA Methylation Regulates Neural Stem Cell Differentiation and Motility. Stem Cell Rep. *8*, 112–124. https://doi.org/10.1016/j.stemcr.2016.11.014.
39. Kogaki, T., Ohshio, I., Ura, H., Iyama, S., Kitae, K., Morie, T., Fujii, S., Sato, S., Nagata, T., Takeda, A.H., et al. (2021). Development of a Highly Sensitive Method for the Quantitative Analysis of Modified Nucleosides Using UHPLC-UniSpray-MS/MS. J. Pharm. Biomed. Anal. *197*, 113943. https://doi.org/10.1016/j.jpba.2021.113943.
40. Songe-Møller, L., van den Born, E., Leihne, V., Vågbø, C.B., Kristoffersen, T., Krokan, H.E., Kirpekar, F., Falnes, P.Ø., and Klungland, A. (2010). Mammalian ALKBH8 Possesses tRNA Methyltransferase Activity Required for the Biogenesis of Multiple Wobble Uridine Modifications Implicated in Translational Decoding. Mol. Cell Biol. *30*, 1814–1827. https://doi.org/10.1128/MCB.01602-09.
41. Saad, A.K., Marafi, D., Mitani, T., Du, H., Rafat, K., Fatih, J.M., Jhangiani, S.N., Coban-Akdemir, Z.; Baylor-Hopkins Center for Mendelian Genomics, and Gibbs, R.A., et al. (2021). Neurodevelopmental Disorder in an Egyptian Family with a Biallelic ALKBH8 Variant. Am. J. Med. Genet. *185*, 1288–1293. https://doi.org/10.1002/ajmg.a.62100.
42. Honda, K., Hase, H., Tanikawa, S., Okawa, K., Chen, L., Yamaguchi, T., Nakai, M., Kitae, K., Ago, Y., Nakagawa, S., and Tsujikawa, K. (2024). ALKBH8 contributes to neurological function through oxidative stress regulation. PNAS nexus *3*, pgae115. https://doi.org/10.1093/pnasnexus/pgae115.
43. Johansson, M.J.O., Esberg, A., Huang, B., Björk, G.R., and Byström, A.S. (2008). Eukaryotic Wobble Uridine Modifications Promote a Functionally Redundant Decoding System. Mol. Cell Biol. *28*, 3301–3312. https://doi.org/10.1128/MCB.01542-07.
44. Cavallin, I., Bartosovic, M., Skalicky, T., Rengaraj, P., Demko, M., Schmidt-Dengler, M.C., Drino, A., Helm, M., and Vanacova, S. (2022). HITS-CLIP Analysis of Human ALKBH8 Reveals Interactions with Fully Processed Substrate tRNAs and with Specific Noncoding RNAs. RNA *28*, 1568–1581. https://doi.org/10.1261/rna.079421.122.
45. Baron, M.H., Isern, J., and Fraser, S.T. (2012). The Embryonic Origins of Erythropoiesis in Mammals. Blood *119*, 4828–4837. https://doi.org/10.1182/blood-2012-01-153486.
46. Socolovsky, M., Murrell, M., Liu, Y., Pop, R., Porpiglia, E., and Levchenko, A. (2007). Negative Autoregulation by FAS Mediates Robust Fetal Erythropoiesis. PLoS Biol. *5*, e252. https://doi.org/10.1371/journal.pbio.0050252.
47. Kresoja-Rakic, J., and Santoro, R. (2019). Nucleolus and rRNA Gene Chromatin in Early Embryo Development. Trends Genet. *35*, 868–879. https://doi.org/10.1016/j.tig.2019.06.005.
48. Bernstein, R.M., and Mukherjee, B.B. (1972). Control of nuclear RNA Synthesis in 2-Cell and 4-Cell Mouse Embryos. Nature *238*, 457–459. https://doi.org/10.1038/238457a0.
49. Rapino, F., Delaunay, S., Zhou, Z., Chariot, A., and Close, P. (2017). tRNA Modification: Is

Cancer Having a Wobble? Trends Cancer *3*, 249–252. https://doi.org/10.1016/j.trecan.2017.02.004.

50. van den Born, E., Vågbø, C.B., Songe-Møller, L., Leihne, V., Lien, G.F., Leszczynska, G., Malkiewicz, A., Krokan, H.E., Kirpekar, F., Klungland, A., and Falnes, P.Ø. (2011). ALKBH8-Mediated Formation of a Novel Diastereomeric Pair of Wobble Nucleosides in Mammalian tRNA. Nat. Commun. *2*, 172. https://doi.org/10.1038/ncomms1173.
51. Endres, L., Begley, U., Clark, R., Gu, C., Dziergowska, A., Małkiewicz, A., Melendez, J.A., Dedon, P.C., and Begley, T.J. (2015). Alkbh8 Regulates Selenocysteine-Protein Expression to Protect against Reactive Oxygen Species Damage. PLoS One *10*, e0131335. https://doi.org/10.1371/journal.pone.0131335.
52. Maddirevula, S., Alameer, S., Ewida, N., de Sousa, M.M.L., Bjørås, M., Vågbø, C.B., and Alkuraya, F.S. (2022). Insight into ALKBH8-related intellectual developmental disability based on the first pathogenic missense variant. Hum. Genet. *141*, 209–215. https://doi.org/10.1007/s00439-021-02391-z.
53. Lee, M.Y., Leonardi, A., Begley, T.J., and Melendez, J.A. (2020). Loss of epitranscriptomic control of selenocysteine utilization engages senescence and mitochondrial reprogramming. Redox Biol. *28*, 101375. https://doi.org/10.1016/j.redox.2019.101375.
54. Brzezicha, B., Schmidt, M., Makalowska, I., Jarmolowski, A., Pienkowska, J., and Szweykowska-Kulinska, Z. (2006). Identification of human tRNA:m5C methyltransferase catalysing intron-dependent m5C formation in the first position of the anticodon of the pre-tRNA Leu (CAA). Nucleic Acids Res. *34*, 6034–6043. https://doi.org/10.1093/nar/gkl765.
55. Auxilien, S., Guérineau, V., Szweykowska-Kulińska, Z., and Golinelli-Pimpaneau, B. (2012). The human tRNA m (5) C methyltransferase Misu is multisite-specific. RNA Biol. *9*, 1331–1338. https://doi.org/10.4161/rna.22180.
56. Hughes, L.A., Rudler, D.L., Siira, S.J., McCubbin, T., Raven, S.A., Browne, J.M., Ermer, J.A., Rientjes, J., Rodger, J., Marcellin, E., et al. (2023). Copy Number Variation in tRNA Isodecoder Genes Impairs Mammalian Development and Balanced Translation. Nat. Commun. *14*, 2210. https://doi.org/10.1038/s41467-023-37843-9.
57. Yien, Y.Y., and Perfetto, M. (2022). Regulation of Heme Synthesis by Mitochondrial Homeostasis Proteins. Front. Cell Dev. Biol. *10*, 895521. https://doi.org/10.3389/fcell.2022.895521.
58. Björk, G.R., Wikström, P.M., and Byström, A.S. (1989). Prevention of Translational Frameshifting by the Modified Nucleoside 1-Methylguanosine. Science *244*, 986–989. https://doi.org/10.1126/science.2471265.
59. Alexandrov, A., Chernyakov, I., Gu, W., Hiley, S.L., Hughes, T.R., Grayhack, E.J., and Phizicky, E.M. (2006). Rapid tRNA Decay Can Result from Lack of Nonessential Modifications. Mol. Cell *21*, 87–96. https://doi.org/10.1016/j.molcel.2005.10.036.
60. Agris, P.F., Vendeix, F.A.P., and Graham, W.D. (2007). tRNA's Wobble Decoding of the Genome: 40 Years of Modification. J. Mol. Biol. *366*, 1–13. https://doi.org/10.1016/j.jmb.2006.11.046.
61. Cui, L., Ma, R., Cai, J., Guo, C., Chen, Z., Yao, L., Wang, Y., Fan, R., Wang, X., and Shi, Y. (2022). RNA modifications: importance in immune cell biology and related diseases. Signal Transduct. Target. Ther. *7*, 334. https://doi.org/10.1038/s41392-022-01175-9.
62. Benak, D., Benakova, S., Plecita-Hlavata, L., and Hlavackova, M. (2023). The role of m6A and m6Am RNA modifications in the pathogenesis of diabetes mellitus. Front. Endocrinol. *14*, 1223583. https://doi.org/10.3389/fendo.2023.1223583.
63. Yarham, J.W., Lamichhane, T.N., Pyle, A., Mattijssen, S., Baruffini, E., Bruni, F., Donnini, C., Vassilev, A., He, L., Blakely, E.L., et al. (2014). Defective i6A37 Modification of Mitochondrial and Cytosolic tRNAs Results from Pathogenic Mutations in TRIT1 and Its Substrate tRNA. PLoS Genet. *10*, e1004424. https://doi.org/10.1371/journal.pgen.1004424.
64. Gingold, H., Tehler, D., Christoffersen, N.R., Nielsen, M.M., Asmar, F., Kooistra, S.M., Christophersen, N.S., Christensen, L.L., Borre, M., Sørensen, K.D., et al. (2014). A dual program for translation regulation in cellular proliferation and differentiation. Cell *158*, 1281–1292. https://doi.org/10.1016/j.cell.2014.08.011.
65. Monies, D., Vågbø, C.B., Al-Owain, M., Alhomaidi, S., and Alkuraya, F.S. (2019). Recessive Truncating Mutations in ALKBH8 Cause Intellectual Disability and Severe Impairment of Wobble Uridine Modification. Am. J. Hum. Genet. *104*, 1202–1209. https://doi.org/10.1016/j.ajhg.2019.03.026.
66. Dewez, M., Bauer, F., Dieu, M., Raes, M., Vandenhaute, J., and Hermand, D. (2008). The conserved Wobble uridine tRNA thiolase Ctu1-Ctu2 is required to maintain genome integrity. Proc. Natl. Acad. Sci. USA *105*, 5459–5464. https://doi.org/10.1073/pnas.0709404105.
67. Shaheen, R., Al-Salam, Z., El-Hattab, A.W., and Alkuraya, F.S. (2016). The syndrome dysmorphic facies, renal agenesis, ambiguous genitalia, microcephaly, polydactyly and lissencephaly (DREAM-PL): Report of two additional patients. Am. J. Med. Genet. *170*, 3222–3226. https://doi.org/10.1002/ajmg.a.37877.
68. Dedon, P.C., and Begley, T.J. (2022). Dysfunctional tRNA reprogramming and codon-biased translation in cancer. Trends Mol. Med. *28*, 964–978. https://doi.org/10.1016/j.molmed.2022.09.007.
69. Chan, P.P., and Lowe, T.M. (2016). GtRNAdb 2.0: an expanded database of transfer RNA genes identified in complete and draft genomes. Nucleic Acids Res. *44*, D184–D189. https://doi.org/10.1093/nar/gkv1309.
70. Tyanova, S., Temu, T., Sinitcyn, P., Carlson, A., Hein, M.Y., Geiger, T., Mann, M., and Cox, J. (2016). The Perseus computational platform for comprehensive analysis of (prote)omics data. Nat. Methods *13*, 731–740. https://doi.org/10.1038/nmeth.3901.
71. Kuleshov, M.V., Jones, M.R., Rouillard, A.D., Fernandez, N.F., Duan, Q., Wang, Z., Koplev, S., Jenkins, S.L., Jagodnik, K.M., Lachmann, A., et al. (2016). Enrichr: a comprehensive gene set enrichment analysis web server 2016 update. Nucleic Acids Res. *44*, W90–W97. https://doi.org/10.1093/nar/gkw377.
72. Ge, S.X., Jung, D., and Yao, R. (2020). ShinyGO: a graphical gene-set enrichment tool for animals and plants. Bioinformatics *36*, 2628–2629. https://doi.org/10.1093/bioinformatics/btz931.
73. Ayres-Silva, J.d.P., Manso, P.P.d.A., Madeira, M.R.d.C., Pelajo-Machado, M., and Lenzi, H.L. (2011). Sequential morphological characteristics of murine fetal liver hematopoietic microenvironment in Swiss Webster mice. Cell Tissue Res. *344*, 455–469. https://doi.org/10.1007/s00441-011-1170-1.

STAR★METHODS

KEY RESOURCES TABLE

REAGENT or RESOURCE	SOURCE	IDENTIFIER
Antibodies		
APC anti-mouse TER-119/Erythroid Cells Antibody	Biolegend	Cat#116211 RRID:AB_313713
PE anti-mouse CD71 Antibody	Biolegend	Cat#113807 RRID:AB_313568
APC Rat IgG2b, κ Isotype Ctrl Antibody	Biolegend	Cat#400611 RRID:AB_326555
PE Rat IgG2a, κ Isotype Ctrl Antibody	Biolegend	Cat#400507 RRID:AB_326530
FITC anti-mouse CD41 Antibody	Biolegend	Cat#133903 RRID:AB_2129746
FITC anti-mouse/human CD45R/B220 Antibody	Biolegend	Cat#103205 RRID:AB_312991
FITC anti-mouse CD3ε Antibody	Biolegend	Cat#100305 RRID:AB_312671
FITC anti-mouse/human CD11b Antibody	Biolegend	Cat#101205 RRID:AB_312788
FITC anti-mouse Ly-6G/Ly-6C (Gr-1) Antibody	Biolegend	Cat#108405 RRID:AB_313370
TruStain FcX™ PLUS (anti-mouse CD16/32) Antibody	Biolegend	Cat#156604 RRID:AB_2783137
Chemicals, peptides, and recombinant proteins		
RNAlater™ Stabilization Solution	Thermo Fisher SCIENTIFIC	Cat#AM7020
QIAzol Lysis Reagent	QIAGEN	Cat#79306
Nuclease P1	FUJIFILM Wako	Cat#145-08221
Alkaline Phosphatase (E. coli C75) (BAP)	TaKaRa	Cat#2120A
Chloroform	FUJIFILM Wako	Cat#033-08631
Ultrapure Water	FUJIFILM Wako	Cat#214-01301
Ammonium bicarbonate	FUJIFILM Wako	Cat#017-02875
Deoxycholic Acid Sodium Salt Monohydrate	Nacarai tesque	Cat#10712-12
N-Lauroylsarcosine Sodium Salt	Nacarai tesque	Cat#20117-12
50 x Protease inhibitor cocktail, Complete EDTA-free	Roche	Cat#11873580001
10 x PhosSTOP Phosphatase Inhibitor Cocktail	Roche	Cat#04906845001
TCEP	Thermo Fisher SCIENTIFIC	Cat#77720
Iodoacetamide	Thermo Fisher SCIENTIFIC	A39271
Trypsin	Thermo Fisher SCIENTIFIC	Cat#90058
Methanol	FUJIFILM Wako	Cat#134-14523
TFA	FUJIFILM Wako	Cat#204-02743
eBioscience™ 7-AAD Viability Staining Solution	Invitrogen™	Cat#00-6993-50
eBioscience™ Flow Cytometry Staining Buffer	Invitrogen™	Cat#00-4222-57
MethoCult complete medium	StemCell Technologies	Cat#M3434

(*Continued on next page*)

Continued

REAGENT or RESOURCE	SOURCE	IDENTIFIER
Critical commercial assays		
Extraction Solution Molecular Biology	Sigma	Cat#E7526
Tissue Preparation Solution	Sigma	Cat#T3073
Neutralization Solution B	Sigma	Cat#N3910
KOD FX	TOYOBO	Cat#KFX-101
Experion™ RNA StdSens and HighSens Analysis Kits	BIO-RAD	Cat#700–7103, #700-7105
Small quality was assessed using an Agilent Small RNA Kit	Agilent	Cat#5067-1548
miRNeasy Micro Kit	QIAGEN	Cat#217084
SuperScript™ VILO™ Master Mix	Thermo Fisher SCIENTIFIC	Cat#11755050
THUNDERBIRD® SYBR™ qPCR Mix	TOYOBO	QPS-201
Flexi® Rabbit Reticulocyte Lysate System	Promega	Cat#L4540
Luciferase Assay Reagent	Promega	Cat#E1483
BCA Protein Assay	Thermo Fisher SCIENTIFIC	Cat#23227
Clariom™ S Pico Assay, mouse	Thermo Fisher SCIENTIFIC	Cat#902933
Software and algorithms		
EASY-nLC 1000 Liquid Chromatograph	Thermo Fisher SCIENTIFIC	RRID: SCR_014993
Thermo Scientific Orbitrap Eclipse Tribrid mass spectrometer	Thermo Fisher SCIENTIFIC	RRID: SCR_023618
DIA-NN	Demichev, Ralser, and Lilley labs	RRID: SCR_022865
Perseus	Max-Planck-Institute of Biochemistry	RRID: SCR_015753
Enrichr	the Ma'ayan Lab	RRID: SCR_001575
ShinyGO	South Dakota State University	RRID: SCR_019213
BD FACS Aria II	BD Biosciences	RRID: SCR_018091
FlowJo	BD Biosciences	RRID: SCR_008520
BZ-X700 microscope	KEYENCE	RRID: SCR_016979
GraphPad Prism	GraphPad Software	RRID: SCR_002798
Qubit 3.0 Fluorometer	Thermo Fisher SCIENTIFIC	RRID:SCR_020311
Transcriptome Analysis Console	Thermo Fisher SCIENTIFIC	RRID:SCR_016519
Deposited data		
Proteome analysis data	this paper	jPOST ID: JPST002999
tRNA-seq analysis data	this paper	PRJNA1148054
Microarray data	this paper	GEO:GSE274779

EXPERIMENTAL MODEL AND STUDY PARTICIPANT DETAILS

Animals

All animal experiments were conducted following the Osaka University Animal Committee guidelines and were housed under a 12-h light-dark cycle, provided with a standard diet, and maintained at a constant temperature.

To obtain WT embryos (MII oocyte, pronucleus, 2-cell, morula, blastocyst, E 10.5, 13.5, 16.5, 19.5, and P0), ovulation induction was performed to 8–16 weeks old female mice. The ovulation induction procedure involved administering 0.1 mL–0.2 mL of CARD HyperOva (KYUDO CO.,LTD) intraperitoneally per mouse, followed by an intraperitoneal injection of 7.5 IU of hCG (123-00078-9, ASKA Pharmaceutical Co., Ltd.) 48 h later. 8–16 weeks old male mice were caged individually before injecting female mice. Male and female mice were co-housed for post ovulation (15–19 h after hCG injection). After co-housing, the vaginal plug was observed to confirm whether the male and female mice had copulated. The female mice in which a plug was confirmed were euthanized on the same day, and MII oocytes and pronuclei were obtained from the ampulla of the oviduct.

Alkbh8-KO mice were generated by deleting the third and fourth exons of *Alkbh8* as previously described.[42] *Alkbh8*-KO mice were bred with C57BL/6N mice through over 10 generations of backcrossing, and the resulting mice were used in the experiments.

To obtain E10.5, 13.5, 19,5 embryos and P0 offsprings, 8–16 weeks old *Alkbh8*-HKO male and female mice were naturally mated in the evening, . The morning after mating, the presence of a vaginal plug was confirmed in female mice. The plug-confirmation day was defined as E0.5. WT and *Alkbh8*-KO mice were compared using littermate pairs.

The sex of the embryos in this study is unknown, because it is challenging to determine the sex of embryos and P0 through observation.

Embryo culture

The MII oocyte and pronucleus produced by copulation were washed in 100-μL KSOM (ARK Resource) drops twice and incubated at 37°C, 5% CO2. The collection of 2-cell embryos, morula, and blastocysts were counted at 24, 48, and 72 h after iThe plug-confirmation day.

METHOD DETAILS

Genotyping

Mouse genotyping was performed by PCR using genomic DNA extracted from the tail. Approximately 5 mm of the mouse tail tip was prepared and placed in a 1.5 mL tube. Then, 100 μL of Extraction Solution Molecular Biology (Sigma, E7526) and 25 μL of Tissue Preparation Solution (Sigma, T3073) were added. After heat treatment at 55°C for 10 min, 100 μL of Neutralization Solution B (Sigma, N3910) was added for neutralization. This solution served as the genomic DNA.

PCR was conducted using 1 μL of the supernatant after centrifugation. A T100TM Thermal Cycler (Bio-Rad) was used for PCR with KOD FX DNA polymerase (TOYOBO). The enzyme solution, containing a final concentration of 0.3 μM for each primer and 0.25 μL of DNA polymerase, was mixed with 1 μL of the measured sample to prepare a 15 μL reaction solution. PCR primers specific to the target sequences were designed. Electrophoresis was performed using a 2% agarose gel.

In vitro fertilization-embryo transfer (IVF-ET)

The experiment was conducted at the Osaka University Institute of Microbial Diseases. In the current study, *in vitro* fertilization was performed using sperm from *Alkbh8*-KO male mice and eggs from *Alkbh8*-HKO female mice. The fertilized embryos were transplanted into the uteri of WT ICR mice for offspring acquisition.

RNA extraction from animal tissues

For mouse embryos, the entire body tissue was immersed in RNA later RNA Stabilization Reagent (QIAGEN) and kept at 4°C for one day for permeation. Subsequently, the tissues were placed in 2 mL screw-cap tubes containing zirconia beads (WATSON), and 700 μL of QIAzol (QIAGEN) was added. The tissues were then homogenized twice using a cell-disruption device (Micro Smash MS-100, TOMY SEIKO) at 2800 rpm for 30 s. Following homogenization, RNA was extracted according to the total RNA or large/small RNA protocols of the miRNeasy Mini Kit (QIAGEN). The extracted RNA was stored at −80°C until used for the next experiment. RNA concentration was measured using a microvolume spectrophotometer (BioSpec-nano, SHIMADZU). Small amounts of RNA were measured using Qubit 3.0 (Thermo Fisher Scientific). Total RNA quality was assessed using the Experion RNA Standard Sens or High Sens Analysis Kit (Bio-Rad). Small RNA quality was assessed using an Agilent Small RNA Kit (Agilent).

Quantification of RNA nucleosides

RNA modification analysis was performed as previously described.[39] Briefly, 50 ng large/small RNA (200 ng) was degraded into nucleosides. To a 30 μL RNA solution, 2′-dG15N5 (Cambridge Isotope Laboratories) was added to a final concentration of 1/100 of the RNA amount as an internal standard.

A solution containing 0.5 U/μL Nuclease P1 (FUJIFILM Wako) diluted five times with DNase/RNase-free H_2O, and an equimolar solution of 0.1 M ammonium acetate (pH 5.3) was added to the RNA solution in 10 μL increments, followed by a 2-h reaction at 45°C. Subsequently, a solution of 0.5 U/μL BAP (TaKaRa Alkaline Phosphatase, *E. coli* C75) diluted 50 times with DNase/RNase-free H_2O was added in 5 μL increments, and the reaction was carried out at 37°C for 2 h.

Afterward, 60 μL of DNase/RNase-free H_2O and 20 μL of chloroform (FUJIFILM Wako) were added, vortexed, and centrifuged at 5000 ×g for 5 min. After centrifugation, the supernatant was transferred to a new 1.5 mL tube and evaporated to dryness. The sample was then reconstituted to a 10 ng/μL concentration using HPLC-grade ultrapure water (FUJIFILM Wako). For measurements, samples were diluted to 1 ng/μL for modified nucleoside detection and 0.01 ng/μL for unmodified nucleoside detection. Heatmap generation and clustering analyses were performed using the ClustVis software (https://biit.cs.ut.ee/clustvis/).

qPCR

Following the manufacturer's instructions, cDNA was synthesized using SuperScriptTM VILOTM Master Mix (Invitrogen). PCR used a Light Cycler 96 (Roche Diagnostics) and THUNDERBIRD SYBR qPCR Mix (TOYOBO) as the DNA polymerase. A total reaction volume of 10 μL was prepared, including 5 μL of DNA polymerase and an enzyme solution containing 0.2 μM final concentration of each primer. For the standard curve or measurement samples, 1 μL was added to the reaction mixture. The qPCR primer sequences used in this study are shown in Figure S6B. Primer sequences and PCR conditions are described below. In addition, measurements of the internal standards *H2afz* and *Ywhaz* were conducted.

Microarray

Total RNA (2 ng) extracted from pronuclear, 2-cell, morula, E10.5, and E16.5 stages was used for the microarray. We used Clariom S Pico Assay (Applied Biosystems, 902932) (following the attached documents). Analysis was performed using the TAC Transcriptome Analysis Console (Thermo Fisher Scientific). Plotting was performed using GraphPad Prism 10. The raw data have been deposited in the BioProject repository (ID: GSE274779).

tRNA-seq

The experiments were outsourced and conducted using Filgen Inc. Small RNA extracted from the whole body of Alkbh8 WT/KO mice at E13.5 was diluted to approximately 100 ng/μL, and 20 μL was subjected to analysis.

Data were analyzed with reference to GtRNAdb[69] for mature cytoplasmic tRNA sequences and mitotRNAdb(http://trna.bioinf.uni-leipzig.de/) for mitochondrial tRNA sequences. Expression profiling of tRNA was calculated based on uniquely mapped reads, including mapped reads. We calculated counts per million and conducted a statistical analysis using Perseus software.[70] Potential incorrect identifications and contaminants (identified by site only, "Reverse," and "Potential contaminant" columns) were filtered out. Counts per million were log2-transformed. Data were filtered to have "3" valid values in at least one sample group. The missing values (tRNA not identified in a run) were imputed by creating a normal distribution of random numbers with a width of 0.3 relative to the standard deviation of the measured values and 1.8 standard deviation downshift of the mean, simulating the distribution of low signal values. Data were normalized by subtracting the median values. A heatmap was plotted using GraphBio (http://www.graphbio1.com/en/). The raw data have been deposited in the BioProject repository (ID: PRJNA1148054).

In vitro translation assay

Based on the attached documents of the Flexi Rabbit Reticulocyte Lysate System (Promega), an *in vitro* translation reaction mixture was prepared to contain 7.0 μL Flexi Rabbit Reticulocyte Lysate, 0.1 μL 1 mM Amino Acid Mixture, minus leucine, 0.1 μL 1 mM Amino Acid Mixture, minus methionine, 0.3 μL 2.5 M potassium chloride, 0.2 μL 1 mg/mL luciferase control RNA and 100 ng/2.3 μL small RNA) and incubated at 30°C for 10 min. Subsequently, 2 μL of the *in vitro* translation reaction mixture was added to 40 μL of Luciferase Assay Reagent (Promega), thoroughly mixed, and the luminescence intensity was measured using the EnVision Multilabel Counter (PerkinElmer).

Proteome analysis

WT and *Alkbh8*-KO mouse embryos at E13.5 were placed in a 2 mL screw-cap tube (WATSON) with a 5 mm zirconia bead. One milliliter of 1x PTS buffer (50 mM ammonium bicarbonate, 12 mM deoxycholic acid sodium monohydrate, 12 mM N-lauroylsarcosine sodium salt, and protease and phosphatase inhibitors) was added, and the samples were completely homogenized using a bead cell disruption device (Micro Smash MS-100) at 2800 rpm for 30 s, repeated twice. The homogenate was centrifuged at 16,000 × *g* for 10 min at 4°C, and 900 μL of the supernatant was transferred to a new tube. The samples were diluted 5-fold with 1x PTS buffer, and the protein concentration was measured using the BCA Protein Assay (23227, Thermo Fisher Scientific) according to the manufacturer's instructions.

For further processing, 100 μg of protein was used, and 5 μL of 200 mM TCEP (77720, Thermo Fisher Scientific) was added. The reaction was carried out at 55°C for 1 h. Subsequently, 5 μL of 375 mM iodoacetamide (A39271, Thermo Fisher Scientific) was added, and the reaction was carried out in the dark for 30 min, followed by methanol-chloroform precipitation. Afterward, 2.5 μg of trypsin (90058, Thermo Fisher Scientific) was added for enzyme digestion, and the peptide was quantified using mass spectrometry after adding TFA (204–02743, FUJIFILM Wako) to create a 0.1% TFA solution.

Online LC-MS was performed using an Easy-nLC 1200 system coupled to an Orbitrap Eclipse Tribrid mass spectrometer (Thermo Fisher Scientific). Samples were trapped on a C18 guard-desalting column (Thermo Fisher Scientific, Acclaim PepMap 100, 75 μm m x 2 cm, nanoViper, C18, 5 μm, 100 Å), and separated on a 12 cm long C18 column (Nikkyo Technos, C18, 3 μm, 75 μm × 12 cm). The nanocapillary solvent A consisted of 100% water and 0.1% formic acid, whereas solvent B consisted of 20% water, 80% acetonitrile, and 0.1% formic acid. At a constant flow rate of 0.3 μL/min, the curved gradient went from 6% B up to 31% B, followed by a steep increase to 90% B in 10 min. The eluted peptide samples were analyzed using a data-independent acquisition (DIA) method. For MS1, the m/z was set from 500 to 1100, the mass resolution was 24,000, the AGC target was 500%, the maximum injection time was 50 ms, and the data type was centroid. MS2 was acquired in quadrupole isolation mode with the isolation window set to 10 m/z, 25% HCD collision energy, 120000 mass resolution with Orbitrap detection, 2000% AGC target, maximum injection time, and centroid data type. Raw data files were processed in library-free mode using DIA-NN (version 1.8.1). Trypsin/P allowed for a maximum of one missed cleavage, N-terminal methionine removal for variable modifications, and fixed carbamidomethylation of cysteine. Peptide lengths ranged from 7 to 30 amino acids. The number of precursors ranged from 300 to 1800, and the number of fragment ions ranged from 200 to 1800. Both MS1 and MS2 mass accuracies were set for automatic determination. Protein inference was set to "Protein names (from FASTA)" and the "Heuristic protein inference" option and MBR (between-run) were employed. RT-dependent, robust, high-precision LC (high precision) options were selected for quantification. We calculated counts per million and conducted a statistical analysis using Perseus software.[69] Potential incorrect identifications and contaminants (identified in "Only identified by site," "Reverse," and "Potential contaminant" columns) were filtered out. Protein intensities were log2-transformed. Data were filtered to have "3" valid values in at least one sample group. Missing values (proteins not identified in a run) were imputed by creating a normal distribution of random numbers with a width of 0.3 relative to the standard deviation of the measured values and 1.8 standard deviation

downshift of the mean, simulating the distribution of low signal values. Data were normalized by subtracting the median values. Functional gene ontology and enrichment analysis were performed using the EnrichR online tool (http://amp.pharm.mssm.edu/Enrichr/)[71] and Shiny GO (http://bioinformatics.sdstate.edu/go/).[72] The heatmap was plotted using GraphBio (http://www.graphbio1.com/en/). The MS data have been deposited in the jPOST repository (jPOST ID: JPST002999).

Flow cytometry

The experiment was conducted by referencing previous studies.[46] Briefly, Liver tissues from E13.5 embryos were extracted and placed in a tube containing 500 μL of eBioscience Flow Cytometry Staining Buffer (00-4222-57, Invitrogen). The cells were separated by pipetting. After removing the debris through a mesh, the cells were washed twice with the staining buffer. TruStain FcX PLUS (anti-mouse CD16/32) Antibody (156604, BioLegend) was added to the cells at a 100-fold dilution and incubated at room temperature (20°C–25°C) for 10 min. After incubation, the cells were washed twice with a staining buffer. Antibody was stained; during the antibody staining process, the cells were incubated for 30 min on ice in the dark. After washing twice with Staining Buffer, eBioscience 7-AAD Viability Staining Solution (00-6993-50, Invitrogen) was added at 5 μL per 100 μL, and the reaction proceeded at room temperature for 5 min. Subsequently, a staining buffer was added to a concentration of 1×10^6 cells/500 μL. Measurements were conducted using Aria (BD Biosciences), and the analysis was performed using the FlowJo analysis software.

Pathological analysis

After dissecting at E13.5, the mice were fixed in 10% neutral-buffered formalin. Paraffin blocks were prepared at Applied Medical Research (Osaka, Japan), and histological specimens were prepared and subjected to pathological analysis using hematoxylin and eosin (HE) staining. Pathological analysis was performed according to literature methods.[73]

Colony-forming unit (CFU) assay

The procedure was carried out based on the attached document of StemCell Technologies. Briefly, After single-cell preparation of the fetal liver (E13.5) by pipetting, cells were counted, and 2×10^4 cells were seeded in MethoCult complete medium (StemCell Technologies, M3434). We seeded 3.5mm dishes with 2×10^4 cells from one liver per individual. Colony counting was performed 10 days after seeding and calculated the average value of two dishes as the value for one individual. Images were captured using the BioZero X700 microscope (KEYENCE Japan, Tokyo).

Hematology analysis

Eight-week-old WT and *Alkbh8*-KO mice were bled from the tail vein by making an incision with a scalpel blade (8-3066-17, Feather) while under survival conditions. Approximately 100 μL of blood was collected into EDTA-treated hematocrit capillaries (2909000, Paul Marienfeld) and transferred to 1.5 mL tubes, which were then placed on ice. Before measurement, the samples were vortexed and analyzed using the CBC mode of the XT-2000i automated hematology analyzer (Sysmex).

QUANTIFICATION AND STATISTICAL ANALYSIS

The figure legends show each experiment's sample sizes (n) and statistical analyses. The analysis software used was GraphPad Prism 10. The asterisks are defined in each relevant figure legend, together with the name of the statistical test.